Eigensolutions for Liners in Uniform Mean Flow Ducts

W. Koch*
DFVLR/AVA Institute for Theoretical Fluid Mechanics, Göttingen, West Germany
and
W. Möhring†
Max-Planck-Institut für Strömungsforschung, Göttingen, West Germany

The problem of sound attenuation in a rectangular acoustically lined duct containing uniform mean flow is investigated analytically by means of the generalized Wiener-Hopf technique. For lined sections of finite axial extent uniqueness of the solution is enforced by imposing edge conditions at the liner interfaces. Several possible edge conditions are considered, including the Kutta condition. The corresponding solutions differ by eigensolutions and it is demonstrated that solution methods, like the mode matching and singularity method, imply differing edge conditions. The power attenuation as well as the SPL traces appear to be rather insensitive to the imposed edge conditions but striking differences are observed for the reflection coefficient.

Introduction

THE ducts of modern aircraft turbofan engines commonly are treated with sound absorbent material in order to reduce the internally generated engine noise. To achieve the high noise reduction required by the ever more stringent noise regulations optimization becomes a necessity. Special techniques, such as axial or circumferential liner segmentation, are used or proposed to reach higher attenuation in the relatively short engine ducts. In addition, the inclusion of the acoustic source characteristics is of vital importance in the optimization procedure (Ref. 1). The commonly used procedure is to consider the engine as a system of interacting elements which, based on the modal approach, leads to large matrix equations containing the modal reflection and transmission factors as summarized in the survey paper of Nayfeh et al.[2] In Vaidya's state-of-the-art review[3] a trend to abandon the modal approach is recognizable and Ffowcs Williams[4] argues that for the modern short but large diameter turbofan engines methods such as geometrical acoustics appear to be more appropriate than modal techniques.

While the most relevant approach may be a matter of debate, certain basic questions concerning finite length liners are still unanswered no matter which method is used. One of these questions was formulated by Ffowcs Williams[4] in a chapter heading, namely: "Acoustic liners absorb sound—but do they destabilize the flow?" In this chapter Ffowcs Williams pointed out that the effectively compliant liner surface admits boundary-layer instabilities of a type not permitted on the rigid surface. This becomes more obvious if one considers the "plug" flow approximation for vanishingly thin viscous boundary layers. In this case, the liner is modeled by a vortex sheet separating the uniform flow region in the duct from the no-flow region in the liner. In treating the infinite (i.e., neglecting liner end effects), constant-area duct problem for plug flow, Tester[5] found a *spatially amplified* mode which he identified as instability mode corresponding to the classical Helmholtz instability.

An analogous situation exists for the related instability of a plane or cylindrical vortex sheet shed from the end of a plate or duct with *different* mean flow velocities on each side. Starting with Orszag and Crow[6] and on to Munt[7] and Rienstra[8] considerable advances were made in solving this problem during the past decade. While Munt and others were led to accept the validity of the Kutta condition at the trailing edge by requiring causality of the solution, Rienstra argued that viscous effects constitute the controlling mechanism and causality is not relevant for periodic flows that exist for all time. These viscous effects appear in the form of prescribed edge conditions in the formulation of the corresponding inviscid problem. Thus the acoustic (i.e., pressure) and hydrodynamic (i.e., instability) fields are coupled at the edge via the prescribed edge condition and the latter is ruled by viscous effects.

On the other hand, essentially no spatial amplification was observed in the lined ducts used in practice and the theoretical existence of the instability mode was attributed to the inadequacy of the model. Indeed, almost all investigators treating finite length liners in ducts containing uniform mean flow by means of the mode matching method (cf. Refs. 9-11) do not even mention the instability mode. Despite this their solutions[10,11] are surprisingly close to the experimental results, at least for sound propagation in the downstream direction. Since the mode matching method is based upon the assumption of eigenfunction completeness, the obvious neglect of certain modes left some researchers with a feeling of unease toward the otherwise very effective method.

Therefore, the basic dilemma is that on the one side instability modes definitely exist, while on the other side the experimental results are close to those solutions which neglect these instability modes. Based upon some earlier work of Jones and Morgan,[12] Crighton and Leppington[13] and Rienstra[8] point out that for the related diffraction problems the unstable solution can be obtained from the stable solution by adding an approximate multiple of an instability eigensolution. It appears that eigensolutions are one reason for the above dilemma and the determination of eigensolutions will be a main concern in the present paper. For this purpose we shall employ the Wiener-Hopf technique which seems particularly suitable since the edge conditions, which are closely linked to uniqueness and hence to the eigensolutions of the problem, are explicitly incorporated in the solution procedure.

While linear theory and the appropriate eigensolutions are expected to provide a fairly accurate solution very close to the upstream liner edge, the situation is quite different already a short distance downstream from this edge. Hydrodynamical

Presented as Paper 81-2017 at the AIAA 7th Aeroacoustics Conference, Palo Alto, Calif., Oct. 5-7, 1981; submitted Oct. 16, 1981; revision received May 19, 1982.

*Research Scientist. Member AIAA.

†Research Scientist.

nonlinearities become important and result in a leveling-off of the instabilities. Here we may modify a suggestion of Möhring and Rahman[14] to find an approximate solution. Möhring and Rahman argue that in treating the real problem the nonlinear terms should be included as source terms and, since exponentially growing terms do not occur in reality, these sources are always such that the unstable modes in the causal solution are never excited in the far field (compare also Refs. 15 and 16). Therefore, as a first approximation to the real problem we may set the amplitude of the instability mode equal to zero in the far field solution and assume that the amplitudes of the remaining modes are changed by only negligible amounts. Naturally, before accepting such a crude assumption, a careful experimental verification is necessary. However, in the related duct radiation problem Munt[17,18] showed very good agreement with experiments, even in the region where the instability wave dominates the solution, by simply neglecting the instability wave there while retaining it for the computation of the reflection factors.

Following Munt's example, Nilsson and Brander recently took a similar approach in a series of papers[19,20] concerning the closely related problems of nonlocally reacting liners and sudden area changes in a circular duct. They combined the solutions for single discontinuities in the boundary condition via the matrix formalism. Contrary to this, the finite length model problem is solved directly here for locally reacting liners by means of the generalized Wiener-Hopf technique (cf. Ref. 21).

Formulation of the Model Problem

We shall be concerned with the attenuation of sound by finite length acoustic liners which are mounted on two opposing walls of an otherwise hard walled rectangular flow duct. To eliminate source or duct end effects, the flow duct is assumed to be infinitely long. This model problem is depicted in Fig. 1.

In order to make the problem amenable to analytic treatment, the following simplifying assumptions are used. The mean flow profile is taken to be uniform across the constant area duct (plug flow approximation), thus modeling vanishingly thin boundary layers. It is well known[2] that neglecting the refractive effects of the boundary layer leads to considerable errors especially for sound waves propagating in the direction opposite to the flow. However, this can be remedied by using a refined model of the inviscid mean flow, a refinement which is not necessary for our objective. The liner is assumed to be locally reacting and describable by a uniform impedance boundary condition. A prescribed acoustic duct mode impinges upon this liner from either upstream or downstream resulting in reflected and transmitted waves. These waves are characterized by their modal reflection and transmission factors.

Neglecting viscosity, thermal conductivity, and nonlinear effects a small disturbance velocity potential Φ_0 can be introduced for the flow duct region

$$v_{0_{\text{tot}}} = U_\infty i + v_0, \quad v_0 = \text{grad}_0 \Phi_0$$

which is governed by the convected wave equation

$$a_\infty^2 \nabla^2 \Phi_0 - \frac{\mathrm{D}^2 \Phi_0}{\mathrm{D}t^2} = 0, \quad \frac{\mathrm{D}}{\mathrm{D}t} = \frac{\partial}{\partial t} + U_\infty \frac{\partial}{\partial x_0} \tag{1}$$

The dimensional pressure disturbance p_0 is then

$$p_0 = -p_\infty \frac{\kappa}{a_\infty^2} \frac{\mathrm{D}\Phi_0}{\mathrm{D}t}$$

with κ being the specific heat ratio. Assuming all quantities to vary harmonically in time, i.e.,

$$\Phi_0 = \hat{\Phi}_0 e^{i\omega t}, \quad v_0 = \hat{v}_0 e^{i\omega t}, \quad p_0 = \hat{p}_0 e^{i\omega t}$$

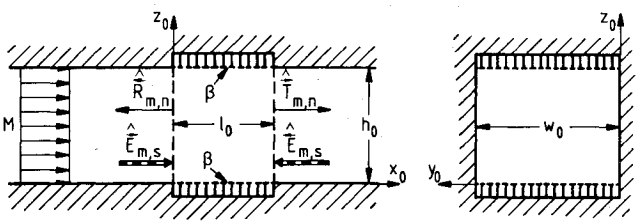

Fig. 1 Finite length liner in a rectangular flow duct.

Eq. (1) can be transformed into the Helmholtz equation

$$\frac{\partial^2 \Phi}{\partial x^2} + \frac{\partial^2 \Phi}{\partial y^2} + \frac{\partial^2 \Phi}{\partial z^2} + K^2 \Phi = 0 \tag{2}$$

for the nondimensional amplitude function Φ if we write

$$\hat{\Phi}_0(x_0, y_0, z_0) = U_\infty L_{\text{ref}} \Phi(x, y, z) e^{iKMx}$$

Here $M = U_\infty / a_\infty$ denotes the mean flow Mach number, $K = K_\infty / \sqrt{1 - M^2}$ is the compressible analogon of the Helmholtz number $K_\infty = \omega L_{\text{ref}} / a_\infty$, and L_{ref} is a reference length (in our case the duct height h_0). At the same time the spatial coordinates are nondimensionalized and transformed by a Prandtl-Glauert type transformation

$$x = x_0 / (L_{\text{ref}} \sqrt{1 - M^2}), \quad y = y_0 / L_{\text{ref}}, \quad z = z_0 / L_{\text{ref}}$$

The corresponding expression for the pressure amplitude $\hat{p}_0$ can be written

$$\hat{p}_0(x_0, y_0, z_0) = p_\infty p(x, y, z) e^{iKMx}$$

$$p = -\frac{\kappa M^2}{\sqrt{1 - M^2}} \left\{ \frac{\partial \Phi}{\partial x} + i \frac{K}{M} \Phi \right\} \tag{3}$$

The boundary condition for the *hard walled section* of the flow duct requires the vanishing of the velocity normal to the bounding wall, i.e.,

$$\frac{\partial \Phi}{\partial z} \left(x, y, \left\{ \begin{matrix} h \\ 0 \end{matrix} \right\} \right) = 0 \text{ for } x < 0 \text{ and } x > l, \quad 0 \le y \le w \tag{4a}$$

$$\frac{\partial \Phi}{\partial y} \left(x, \left\{ \begin{matrix} w \\ 0 \end{matrix} \right\}, z \right) = 0 \quad 0 \le z \le h, \text{ all } x \tag{4b}$$

Here $l = l_0 / (L_{\text{ref}} \sqrt{1 - M^2})$, $h = h_0 / L_{\text{ref}}$, and $w = w_0 / L_{\text{ref}}$ denote the reduced liner length, duct height, and duct width. For the mathematical treatment of the boundary condition in the *soft walled section* $0 \le x \le l$ the liner is modeled by a vortex sheet[22] separating the uniform mean flow region within the duct from the no-flow region in the liner. The impedance boundary condition is then applied on the no-flow side. The two regions are coupled by matching the pressure p_0 and the particle displacement η_0 on either side of the vortex sheet, i.e.,

$$p_0^{(d)} = p_0^{(l)} \tag{5a}$$

$$\eta_0^{(d)} = \eta_0^{(l)} \equiv \eta_0 \tag{5b}$$

Writing

$$\eta_0 = \hat{\eta}_0 e^{i\omega t}, \quad \hat{\eta}_0(x_0, y_0, z_0) = L_{\text{ref}} \eta(x, y, z) e^{iKMx} \tag{6}$$

the normal components v_{0_z} of the acoustic velocities on the liner and the freestream side of the vortex sheet can be ex-

pressed in terms of the particle displacement

$$v_{0_z}^{(l)} = \frac{\partial \eta_0^{(l)}}{\partial t} = i\omega \hat{\eta}_0 e^{i\omega t} \tag{7a}$$

$$v_{0_z}^{(d)} = \frac{\mathrm{D}\eta_0^{(d)}}{\mathrm{D}t} = \left(i\omega + U_\infty \frac{\partial}{\partial x_0}\right)\hat{\eta}_0 e^{i\omega t} \equiv \frac{\partial \Phi_0}{\partial z_0} \tag{7b}$$

Rewriting Eq. (7b) in terms of our nondimensionalized variables we obtain a relation between η and $\partial\Phi/\partial z$ on the boundary

$$\frac{\partial \Phi}{\partial z}\left(x,y,\begin{Bmatrix} h \\ 0 \end{Bmatrix}\right) = \frac{iK_\infty}{M(1-M^2)}\left\{1 + \frac{M}{iK}\frac{\partial}{\partial x}\right\}\eta\left(x,y,\begin{Bmatrix} h \\ 0 \end{Bmatrix}\right) \tag{8}$$

The impedance boundary condition

$$p_0^{(l)} = v_{0_n}^{(l)}/\beta_0 = (\rho_\infty a_\infty/\beta) v_{0_n}^{(l)}$$

together with Eqs. (7a), (6), (5a), and (3) provides the relation

$$\mp \frac{\beta M}{1-M^2}\left\{1 + \frac{M}{iK}\frac{\partial}{\partial x}\right\}\Phi\left(x,y,\begin{Bmatrix} h \\ 0 \end{Bmatrix}\right) = \eta\left(x,y,\begin{Bmatrix} h \\ 0 \end{Bmatrix}\right) \tag{9}$$

between η and Φ on the boundary $0 \le x \le l$. Here, $v_{0_n}^{(l)}$ denotes the normal component of the acoustic velocity pointing into the liner and β_0 is the normal wall admittance of the liner. Eliminating η from Eqs. (8) and (9) the well-known soft wall boundary relation

$$\frac{\partial \Phi}{\partial z}\left(x,y,\begin{Bmatrix} h \\ 0 \end{Bmatrix}\right) = \mp iK_\infty \beta \left\{\left[1 + \frac{M}{iK}\frac{\partial}{\partial x}\right]\Big/[1-M^2]\right\}^{\nu} \Phi\left(x,y,\begin{Bmatrix} h \\ 0 \end{Bmatrix}\right)$$

is recovered, with $\nu = 2$ for continuity of particle displacement and $\nu = 1$ for continuity of particle velocity. However, in our treatment it is advantageous to keep Eqs. (8) and (9).

The introduced boundary conditions permit a separation-of-variables solution such that Φ (as well as p) can be written in the form

$$\Phi(x,y,z) = \sum_{m=0}^{\infty} \Phi_m(x,z)\cos(K_m y), \quad K_m = m\pi/w$$

Since there is no cross coupling between different circumferential modes (index m) the theory can be restricted to a fixed m without loss of generality. Then Eq. (2) becomes

$$\frac{\partial^2 \Phi_m}{\partial x^2} + \frac{\partial^2 \Phi_m}{\partial z^2} + (K^2 - K_m^2)\Phi_m = 0 \tag{10}$$

The formulation of the boundary value problem is completed by requiring that all waves must be outgoing with the exception of the prescribed incident waves (*energy radiation condition*). Furthermore, the solution is rendered unique by imposing certain *edge conditions*. In the present paper we do not prescribe edge conditions a priori but rather look at several possible edge conditions.

Derivation of the Generalized Wiener-Hopf Equation

Practically all analytical methods for the finite length *zero mean flow* case are in accordance with each other and show good agreement with experimental results as long as the sound source and the liner impedance are prescribed with sufficient accuracy. The zero mean flow theory can, therefore, be used with confidence as a solid basis for any further theoretical development. The situation is quite different if mean flow is present. Even for the simple plug flow model the various solution methods do not produce identical results. One reason for these discrepancies is the existence of eigensolutions which are closely linked to the imposed edge conditions. Therefore, a main objective of this paper is to investigate the influence of different edge conditions in order to establish a one to one correspondence between the various solutions and the edge conditions which produce these solutions.

In applying the Wiener-Hopf technique Fourier transforms are required with respect to x. However, due to the unattenuated waves in the hard walled sections, the Fourier transform of Φ_m does not exist. This difficulty can be circumvened, for example, by subtracting all propagating waves for $x<0$. For this purpose the general form of the solution in the hard-walled section is needed and can be found easily by a separation-of-variables procedure in conjunction with the radiation condition. We find for $x<0$

$$\Phi_m(x,z) = \hat{\bar{E}}_{m,s} e^{i\gamma_{m,s}x}\cos(K_s z) + \sum_{n=0}^{N} \hat{\bar{R}}_{m,n} e^{-i\gamma_{m,n}x}\cos(K_n z) + \varphi_m(x,z) \tag{11}$$

and for $x>l$

$$\Phi_m(x,z) = \hat{\bar{E}}_{m,s} e^{-i\gamma_{m,s}x}\cos(K_s z) + \sum_{n=0}^{N} \hat{\bar{T}}_{m,n} e^{i\gamma_{m,n}x}\cos(K_n z) + \psi_m(x,z) \tag{12}$$

Here $\hat{\bar{E}}_{m,s}$ and $\hat{\bar{E}}_{m,s}$ denote the prescribed amplitudes of the unattenuated incident waves impinging from upstream or downstream, respectively (cf. Fig. 1), while $\hat{\bar{R}}_{m,n}$ are the unknown amplitudes of the upstream reflected and $\hat{\bar{T}}_{m,n}$ the unknown amplitudes of the downstream transmitted cut-on waves. φ_m and ψ_m contain all remaining cut-off waves. The hard wall propagation constants are defined by

$$\gamma_{m,n} = -\sqrt{K^2 - K_m^2 - K_n^2} \text{ for } K^2 > K_m^2 + K_n^2$$
$$= i\sqrt{K_m^2 + K_n^2 - K^2} \text{ for } K^2 < K_m^2 + K_n^2 \tag{13}$$

where $K_n = n\pi/h$, $n = 0,1,2,\ldots$. The resonant case $K^2 = K_m^2 + K_n^2$ has to be excluded.

The problem is now formulated in terms of the function φ_m. The Wiener-Hopf equation provides a functional relation between certain unknown boundary functions. In general, these unknown boundary functions comprise the unknown values of the solution function and its normal derivative along the boundary. It is, therefore, advantageous for the formulation of the Wiener-Hopf equation to supplement the known boundary conditions Eqs. (4a) and (9) by unknown functions defined over the remainder of the boundary.

Introducing the unknown displacement functions $\eta_m^{(i),(o)}(x)$ we may write for Eq. (4a) together with Eq. (8)

$$\frac{\partial\varphi_m}{\partial z}\left(x,z=\begin{Bmatrix}h\\0\end{Bmatrix}\right)=0,\quad x<0;\qquad=\frac{iK_\infty}{M(1-M^2)}\left\{1+\frac{M}{iK}\frac{\partial}{\partial x}\right\}\begin{Bmatrix}\eta_m^{(o)}(x),z=h\\ \eta_m^{(i)}(x),z=0\end{Bmatrix},\quad 0<x<l;\qquad=0,\quad x>l \tag{14}$$

Similarly, by introducing the unknown pressure-like functions $g_-^{(i),(o)}(x)$ and $g_+^{(i),(o)}(x)$ and taking account of the definitions Eqs. (11) and (12) we may supplement the boundary condition Eq. (9)

$$\frac{\beta M}{1-M^2}\left\{1+\frac{M}{iK}\frac{\partial}{\partial x}\right\}\varphi_m\left(x,z=\begin{Bmatrix}h\\0\end{Bmatrix}\right)=\begin{Bmatrix}g_-^{(o)}(x),z=h\\ g_-^{(i)}(x),z=0\end{Bmatrix},\quad x<0;\quad=\begin{Bmatrix}-\eta_m^{(o)}(x),z=h\\ +\eta_m^{(i)}(x),z=0\end{Bmatrix}-\frac{\beta M}{1-M^2}R_m\left(x,\begin{Bmatrix}h\\0\end{Bmatrix}\right),\quad 0<x<l;$$

$$=\begin{Bmatrix}g_+^{(o)}(x),z=h\\ g_+^{(i)}(x),z=0\end{Bmatrix}-\frac{\beta M}{1-M^2}\left[R_m\left(x,\begin{Bmatrix}h\\0\end{Bmatrix}\right)-T_m\left(x,\begin{Bmatrix}h\\0\end{Bmatrix}\right)\right],\quad x>l \tag{15}$$

Here, the following abbreviations were used:

$$R_m(x,z)=\left\{1+\frac{M}{iK}\frac{\partial}{\partial x}\right\}\left[\hat{\bar{E}}_{m,s}e^{i\gamma_{m,s}x}\cos(K_sz)+\sum_{n=0}^{N}\hat{\bar{R}}_{m,n}e^{-i\gamma_{m,n}x}\cos(K_nz)\right]=\left[1+\gamma_{m,s}\frac{M}{K}\right]\hat{\bar{E}}_{m,s}e^{i\gamma_{m,s}x}\cos(K_sz)$$

$$+\sum_{n=0}^{N}\left[1-\gamma_{m,n}\frac{M}{K}\right]\hat{\bar{R}}_{m,n}e^{-i\gamma_{m,n}x}\cos(K_nz)$$

$$T_m(x,z)=\left\{1+\frac{M}{iK}\frac{\partial}{\partial x}\right\}\left[\hat{\bar{E}}_{m,s}e^{-i\gamma_{m,s}x}\cos(K_sz)+\sum_{n=0}^{N}\hat{\bar{T}}_{m,n}e^{i\gamma_{m,n}x}\cos(K_nz)\right]=\left[1-\gamma_{m,s}\frac{M}{K}\right]\hat{\bar{E}}_{m,s}e^{-i\gamma_{m,s}x}\cos(K_sz)$$

$$+\sum_{n=0}^{N}\left[1+\gamma_{m,n}\frac{M}{K}\right]\hat{\bar{T}}_{m,n}e^{i\gamma_{m,n}x}\cos(K_nz)$$

When applying the Fourier transformation with respect to x to the governing Eq. (10), which is also satisfied by φ_m and to the boundary conditions Eqs. (14) and (15), one basic requirement is that all interchanges of differential, integration, and limit operations are permitted. This requirement seriously restricts the class of solution functions unless generalized functions are included. For example, $\eta_m(x)$ may contain jumps or $g(x)$ may be nonintegrable at $x=0$ or $x=l$. Therefore, we should be ready to extend the class of solution functions whenever difficulties are encountered.

Defining the Fourier transform of φ_m by

$$\bar{\varphi}_m(z;\xi)=\int_{-\infty}^{\infty}\varphi_m(x,z)e^{-i\xi x}\mathrm{d}x$$

where ξ is the complex Fourier transformation variable, we take the Fourier transformation of Eq. (10)

$$\frac{\mathrm{d}^2\bar{\varphi}_m}{\mathrm{d}z^2}-\gamma^2\bar{\varphi}_m=0,\qquad\gamma=\sqrt{\xi^2+K_m^2-K^2}$$

with the general solution

$$\bar{\varphi}_m(z;\xi)=\alpha_m(\xi)e^{\gamma z}+\beta_m(\xi)e^{-\gamma z} \tag{16}$$

φ_m converges absolutely in the strip $-\mathrm{Im}(\gamma_{m,N+1})<\mathrm{Im}\,\xi<0$ since $\varphi_m\sim\exp(-i\gamma_{m,N+1}x)$ for $x\to-\infty$ and contains the cut-on transmitted waves for $x\to+\infty$. Similarly, the Fourier transformation of the boundary conditions Eqs. (14) and (15) give

$$\frac{\mathrm{d}\bar{\varphi}_m}{\mathrm{d}z}\left(z=\begin{Bmatrix}h\\0\end{Bmatrix};\ \xi\right)=\frac{iK_\infty}{M(1-M^2)}\left(1+\frac{M}{K}\xi\right)\begin{Bmatrix}\bar{\eta}_m^{(o)}(\xi;l)\\ \bar{\eta}_m^{(i)}(\xi;l)\end{Bmatrix}+\frac{1}{\sqrt{1-M^2}}\left(\begin{Bmatrix}\eta_m^{(o)}(l)\\ \eta_m^{(i)}(l)\end{Bmatrix}e^{-i\xi l}-\begin{Bmatrix}\eta_m^{(o)}(0)\\ \eta_m^{(i)}(0)\end{Bmatrix}\right) \tag{17}$$

$$\frac{\beta M}{1-M^2}\left(1+\frac{M}{K}\xi\right)\bar{\varphi}_m\left(z=\begin{Bmatrix}h\\0\end{Bmatrix};\ \xi\right)=\begin{Bmatrix}\bar{g}_\oplus^{(o)}(\xi)-\bar{\eta}_m^{(o)}(\xi;\ l)+e^{-i\xi l}\bar{g}_\ominus^{(o)}(\xi;\ l)\\ \bar{g}_\oplus^{(i)}(\xi)+\bar{\eta}_m^{(i)}(\xi;\ l)+e^{-i\xi l}\bar{g}_\ominus^{(i)}(\xi;\ l)\end{Bmatrix}$$

$$-\frac{\beta M}{1-M^2}\begin{Bmatrix}\bar{R}_m(z=h;\ \xi)-e^{-i\xi l}\bar{T}_m(z=h;\ \xi;\ l)\\ \bar{R}_m(z=0;\ \xi)-e^{-i\xi l}\bar{T}_m(z=0;\ \xi;\ l)\end{Bmatrix} \tag{18}$$

if we explicitly allow particle displacement jumps $\eta_m(0)$ and $\eta_m(l)$ of still unknown magnitude at $x=0,\ l$. Naturally, in this case the left-hand side of Eq. (14) has to be interpreted as a generalized function. Furthermore, the following definitions were introduced:

$$\bar{g}_\oplus^{(i),(o)}(\xi)=\int_{-\infty}^{0}g_-^{(i),(o)}(x)e^{-i\xi x}\mathrm{d}x\qquad\text{holomorphic in Im}\,\xi>-\mathrm{Im}\ (\gamma_{m,N+1}) \tag{19a}$$

$$\bar{\eta}_m^{(i),(o)}(\xi;\ l)=\int_0^l \eta_m^{(i),(o)}(x)e^{-i\xi x}\mathrm{d}x \qquad \text{entire function of } \xi \tag{19b}$$

$$\bar{g}_{\ominus}^{(i),(o)}(\xi;\ l)=\int_l^\infty g_+^{(i),(o)}(x)e^{-i\xi(x-l)}\mathrm{d}x \qquad \text{holomorphic in Im } \xi<\text{Im}(\gamma_{m,N+1}) \tag{19c}$$

$$\bar{R}_m\left(z=\begin{Bmatrix}h\\0\end{Bmatrix};\ \xi\right)=\int_0^\infty R_m\left(x,z=\begin{Bmatrix}h\\0\end{Bmatrix}\right)e^{-i\xi x}\mathrm{d}x=\left[1+\gamma_{m,s}\frac{M}{K}\right]\frac{\hat{\bar{E}}_{m,s}}{i(\xi-\gamma_{m,s})}\begin{Bmatrix}(-1)^s\\1\end{Bmatrix}$$
$$+\sum_{n=0}^{N}\left[1-\gamma_{m,n}\frac{M}{K}\right]\frac{\hat{\bar{R}}_{m,s}}{i(\xi+\gamma_{m,n})}\begin{Bmatrix}(-1)^n\\1\end{Bmatrix} \tag{19d}$$

$$\bar{T}_m\left(z=\begin{Bmatrix}h\\0\end{Bmatrix};\ \xi;\ l\right)=\int_l^\infty T_m\left(x,z=\begin{Bmatrix}h\\0\end{Bmatrix}\right)e^{-i\xi(x-l)}\mathrm{d}x=\left[1-\gamma_{m,s}\frac{M}{K}\right]\frac{\hat{\bar{E}}_{m,s}e^{-i\gamma_{m,s}l}}{i(\xi+\gamma_{m,s})}\begin{Bmatrix}(-1)^s\\1\end{Bmatrix}$$
$$+\sum_{n=0}^{N}\left[1+\gamma_{m,n}\frac{M}{K}\right]\frac{\hat{\bar{T}}_{m,n}e^{i\gamma_{m,n}l}}{i(\xi-\gamma_{m,n})}\begin{Bmatrix}(-1)^n\\1\end{Bmatrix} \tag{19e}$$

By extracting $\exp(-i\xi l)$, $\bar{g}_{\oplus}$ as well as $\bar{g}_{\ominus}$ have algebraic behavior for $|\xi|\to\infty$ in their upper or lower half-plane of holomorphy (indicated by the subscript $\oplus$ or $\ominus$) as can be checked a posteriori.

The integration functions $\alpha(\xi)$ and $\beta(\xi)$ in Eq. (16) can be eliminated in terms of $\bar{\eta}_m^{(i)}$ and $\bar{\eta}_m^{(o)}$ by means of the transformed boundary condition Eq. (17) such that

$$\bar{\varphi}_m(z;\ \xi)=\frac{iK_\infty(1+M\xi/K)}{M(1-M^2)\gamma\sinh(\gamma h)}\{\bar{\eta}_m^{(o)}\cosh(\gamma z)-\bar{\eta}_m^{(i)}\cosh[\gamma(h-z)]\}+\frac{1}{\sqrt{1-M^2}\gamma\sinh(\gamma h)}\{[e^{-i\xi l}\eta_m^{(o)}(l)-\eta_m^{(o)}(0)]\cosh(\gamma z)$$
$$-[e^{-i\xi l}\eta_m^{(i)}(l)-\eta_m^{(i)}(0)]\cosh[\gamma(h-z)]\} \tag{20}$$

Substituting this into the remaining boundary condition Eq. (18) two functional equations are obtained which relate the several unknown functions. These two functional equations can be uncoupled by adding and subtracting them from each other, resulting in two uncoupled generalized Wiener-Hopf equations which correspond to *symmetric* and *antisymmetric* excitation, respectively:

$$\bar{g}_{\oplus}^{(s)}(\xi)-\mathfrak{L}^{(s)}(\xi;\ M)\bar{\eta}_m^{(s)}(\xi)+e^{-i\xi l}\bar{g}_{\ominus}^{(s)}(\xi)=\frac{\beta M}{1-M^2}\{\bar{R}_m^{(s)}-e^{-i\xi l}\bar{T}_m^{(s)}\}+\frac{\beta M(1+M\xi/K)}{(1-M^2)^{3/2}}\frac{\cos(\tilde{\gamma}h/2)}{\tilde{\gamma}\sin(\tilde{\gamma}h/2)}\{\eta_m^{(s)}(0)-e^{-i\xi l}\eta_m^{(s)}(l)\} \tag{21}$$

$$\bar{g}_{\oplus}^{(a)}(\xi)-\mathfrak{L}^{(a)}(\xi;\ M)\bar{\eta}_m^{(a)}(\xi)+e^{-i\xi l}\bar{g}_{\ominus}^{(a)}(\xi)=\frac{\beta M}{1-M^2}\{\bar{R}_m^{(a)}-e^{-i\xi l}\bar{T}_m^{(a)}\}-\frac{\beta M(1+M\xi/K)}{(1-M^2)^{3/2}}\frac{\sin(\tilde{\gamma}h/2)}{\tilde{\gamma}\cos(\tilde{\gamma}h/2)}\{\eta_m^{(a)}(0)-e^{-i\xi l}\eta_m^{(a)}(l)\} \tag{22}$$

These two Wiener-Hopf equations are at first defined only in their respective strip of holomorphy $-\text{Im}(\gamma_{m,N^{(s),(a)}+1})<\text{Im}\,\xi<0$. If we define

$$\gamma=i\tilde{\gamma},\qquad \tilde{\gamma}=\sqrt{K^2-K_m^2-\xi^2}$$

the corresponding kernel functions are

$$\mathfrak{L}^{(s)}(\xi;\ M)=\left[\tilde{\gamma}\sin(\tilde{\gamma}h/2)-i\beta K\sqrt{1-M^2}\left\{\frac{1+M\xi/K}{1-M^2}\right\}^2\cos(\tilde{\gamma}h/2)\right]\Big/\tilde{\gamma}\sin(\tilde{\gamma}h/2)$$

$$\mathfrak{L}^{(a)}(\xi;\ M)=\left[\tilde{\gamma}\cos(\tilde{\gamma}h/2)+i\beta K\sqrt{1-M^2}\left\{\frac{1+M\xi/K}{1-M^2}\right\}^2\sin(\tilde{\gamma}h/2)\right]\Big/\tilde{\gamma}\cos(\tilde{\gamma}h/2)$$

The symmetric and antisymmetric contributions, corresponding to symmetric and antisymmetric excitation, are defined by

$$\bar{g}_{\oplus}^{(o)}+\bar{g}_{\oplus}^{(i)}=2\bar{g}_{\oplus}^{(s)},\qquad \bar{g}_{\ominus}^{(o)}+\bar{g}_{\ominus}^{(i)}=2\bar{g}_{\ominus}^{(s)}$$

$$\bar{g}_{\oplus}^{(o)}-\bar{g}_{\oplus}^{(i)}=2\bar{g}_{\oplus}^{(a)},\qquad \bar{g}_{\ominus}^{(o)}-\bar{g}_{\ominus}^{(i)}=2\bar{g}_{\ominus}^{(a)}$$

$$\bar{\eta}_m^{(o)}-\bar{\eta}_m^{(i)}=2\bar{\eta}_m^{(s)},\qquad \bar{\eta}_m^{(o)}+\bar{\eta}_m^{(i)}=2\bar{\eta}_m^{(a)}$$

$$\bar{R}_m(z=h)+\bar{R}_m(z=0)=2\bar{R}_m^{(s)},$$

$$\bar{T}_m(z=h)+\bar{T}_m(z=0)=2\bar{T}_m^{(s)}$$

$$\bar{R}_m(z=h)-\bar{R}_m(z=0)=2\bar{R}_m^{(a)},$$

$$\bar{T}_m(z=h)-\bar{T}_m(z=0)=2\bar{T}_m^{(a)}$$

For $M=0$ the kernel functions reduce to the ones for zero mean flow (cf. Ref. 23). From now on we shall deal explicitly only with the symmetric problem (21) since the solution procedure for the antisymmetric problem (22) is exactly the same.

Solution of the Model Problem

Multiplicative Kernel Factorization

The *first step* in solving the Wiener-Hopf Eq. (21) is the *multiplicative factorization* of $\mathcal{L}^{(s)}$ into two functions $\mathcal{L}^{(s)}_{\oplus}$ and $\mathcal{L}^{(s)}_{\ominus}$ which are holomorphic, nonzero, and grow algebraically as $|\xi| \to \infty$ in an upper or lower half-plane, i.e.,

$$\mathcal{L}^{(s)}(\xi;M) = \mathcal{L}^{(s)}(\xi;M)_{\oplus}\,\mathcal{L}^{(s)}(\xi;M)_{\ominus} \tag{23}$$

Due to the lateral boundedness of the model problem $\mathcal{L}^{(s)}$ has only zeros and poles but no branch points. Therefore, Weierstrass' infinite product theorem (cf. Ref. 21, p. 15) may be used to express the numerator and denominator of $\mathcal{L}^{(s)}$ in terms of infinite products which can then be associated with the respective half-plane.

The *poles* of $\mathcal{L}^{(s)}$ are identified easily as the hard wall symmetric eigenvalues, cf. Eq. (13)

$$\xi = \pm\gamma_{m,2n}, \qquad n=0,1,2,\ldots$$

a finite number of which is real, corresponding to the unattenuated duct waves, while all others are purely imaginary. Assuming temporarily that the system is slightly damped corresponding to K having a small but negative imaginary part [for the chosen time factor $\exp(+i\omega t)$] it is easy to identify all poles $\xi = +\gamma_{m,2n}$ as lying in the $\oplus$ plane.

The *zeros* of $\mathcal{L}^{(s)}$ correspond to the soft wall eigenvalues and are best studied in the complex $\tilde{\gamma}$ plane with $\xi = \pm(K^2 - K_m^2 - \tilde{\gamma}^2)^{1/2}$. Consistent with the two signs of the square root, two distinct sequences of infinitely many zeros are obtained. Denoting the zeros in the $\tilde{\gamma}$ plane corresponding to the plus sign of the square root by λ^{+}_{2n} and the ones corresponding to the minus sign by λ^{-}_{2n} one can write for the zeros of $\mathcal{L}^{(s)}$ in the ξ plane

$$\xi = \pm\lambda^{+}_{m,2n} \equiv \pm\sqrt{K^2 - K_m^2 - \lambda^{\pm 2}_{2n}}$$

The roots $\lambda^{\pm}_{2n}$ are complex but since $\mathcal{L}^{(s)}$ is an even function of $\tilde{\gamma}$, the search procedure may be limited to the right half of the $\tilde{\gamma}$ plane. Also, for convenience in the computer program and as long as K is real, the value of the square root may be fixed by using the principal value (P.V.), i.e.,

$$\sqrt{K^2 - K_m^2 - \tilde{\gamma}^2}$$

$$= -\text{P.V.}\sqrt{K^2 - K_m^2 - \tilde{\gamma}^2} \quad \text{if } \operatorname{Im}(\tilde{\gamma}) > 0, \quad \operatorname{Re}(\tilde{\gamma}) > 0$$

$$= +\text{P.V.}\sqrt{K^2 - K_m^2 - \tilde{\gamma}^2} \quad \text{if } \operatorname{Im}(\tilde{\gamma}) < 0, \quad \operatorname{Re}(\tilde{\gamma}) > 0$$

One basic problem is which numbers the index n may take. In studies using the mode matching technique it is customary to compute the λ_{2n} iteratively with either the hard wall eigenvalues (cf. Ref. 10) or the zero Mach number eigenvalues (cf. Ref. 11) as starting values in the numerical procedure. This establishes a one to one correspondence between the hard wall or zero Mach number eigenvalues on the one side, and the uniform mean flow eigenvalues on the other side, such that n would start with $n=0$. However, if the split functions $\mathcal{L}^{(s)}_{\oplus}$ and $\mathcal{L}^{(s)}_{\ominus}$ are evaluated numerically by using only these zeros, their behavior for $|\xi| \to \infty$ is exponential and multiplied together they do not result in $\mathcal{L}^{(s)}$ as they should. The only possible cause for this discrepancy is that some modes are missing. Indeed, prior to this investigation, Eversman[24] already found two extra eigenvalues [corresponding to the two signs of the square root $(K^2 - K_m^2 - \tilde{\gamma}^2)^{1/2}$] for admittances with a positive imaginary part. Hence, different from the $M=0$ case, the index n for the zeros of $\mathcal{L}^{(s)}$ for $M \neq 0$ starts with $n=-1$. For the actual numerical evaluation of the zeros Eversman's powerful root finding eigenvalue routine (cf. Ref. 24) was of immense help and played an important part in performing this investigation.

Mathematically, the appearance of the additional modes can be traced to the factor $(1+M\xi/K)^2$ which multiplies β in $\mathcal{L}^{(s)}$ as noted by Tester.[5] Tester also realized their physical significance as being the compressible counterparts of Helmholtz instability waves. This leads us to the second problem, namely, the correct multiplicative factorization of $\mathcal{L}^{(s)}$. If K is real, or at least with only a small negative imaginary part, the two additional zeros (boxed in values in Fig. 2) belong to different half-planes and application of Weierstrass' infinite product theorem gives for K almost real

$$\mathcal{L}^{(s)}(\xi;M)_{\oplus} = \mathcal{L}^{(s)}(0)\,(1+\xi/\lambda^{-}_{m,-2}) \prod_{n=0}^{\infty} \frac{1+\xi/\lambda^{-}_{m,2n}}{1+\xi/\gamma_{m,2n}} \tag{24a}$$

$$\mathcal{L}^{(s)}(\xi;M)_{\ominus} = (1-\xi/\lambda^{+}_{m,-2}) \prod_{n=0}^{\infty} \frac{1-\xi/\lambda^{+}_{m,2n}}{1-\xi/\gamma_{m,2n}} \tag{24b}$$

where $\mathcal{L}^{(s)}(0) = \mathcal{L}^{(s)}(\xi;M)$ evaluated at $\xi=0$. The exponential factors in the infinite products cancel each other, thus ensuring algebraic behavior of $\mathcal{L}^{(s)}_{\oplus}$ and $\mathcal{L}^{(s)}_{\ominus}$ for $|\xi| \to \infty$ in the respective half-plane of holomorphy.

Based upon the asymptotic expansions for $n \gg 1 (M \neq 0)$

$$\lambda^{\pm}_{m,2n} \sim i\frac{2n\pi}{h}\left\{1 + \frac{c_1}{2n} + \frac{c_2}{(2n)^2} + \frac{c_3^{\pm}}{(2n)^3} + \ldots\right\}$$

$$c_1 = 1; \quad c_2 = c_0 - \frac{h^2(K^2 - K_m^2)}{2\pi^2}; \quad c_0 = \frac{2hK(1-M^2)^{3/2}}{i\beta M^2\pi^2}$$

$$c_3^{\pm} = -c_0\left(1 \pm \frac{2hK}{iM\pi}\right) + \frac{h^2(K^2 - K_m^2)}{2\pi^2}$$

standard asymptotic methods (cf. Ref. 21, p. 128) provide the estimates

$$\mathcal{L}^{(s)}(\xi;M)_{\oplus} \sim \xi^{1/2} \text{ as } |\xi| \to \infty \text{ in the } \oplus \text{ plane} \tag{25a}$$

$$\mathcal{L}^{(s)}(\xi;M)_{\ominus} \sim \xi^{1/2} \text{ as } |\xi| \to \infty \text{ in the } \ominus \text{ plane} \tag{25b}$$

The preceding asymptotic expansion for $\lambda^{\pm}_{m,2n}$ suggests the ordering of the numerically computed eigenvalues for real K according to the magnitude of their imaginary parts. It is also evident that the above asymptotic expansions are nonuniform, particularly with regard to M and K.

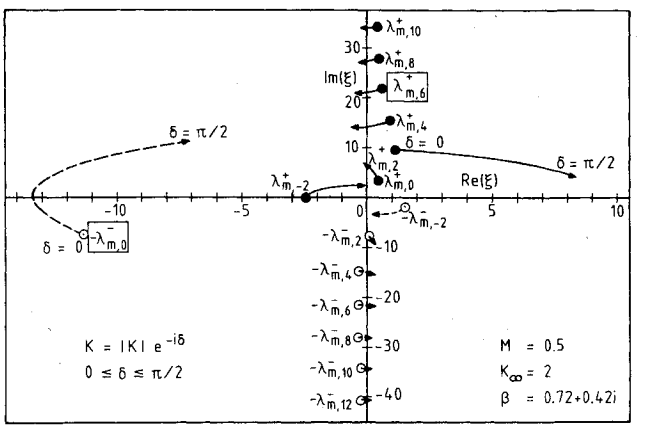

Fig. 2 Axial eigenvalues $\lambda^{\pm}_{m,2n}$ for complex K.

Proceeding as just described, no account is taken of possible instability modes and the corresponding solution is the conventional stable solution. In order to include instability modes in a Fourier transformation solution, a commonly used procedure is to consider K complex, i.e., $K=|K|\exp(-i\delta)$ with δ close to $\pi/2$. Analytic continuation arguments are then used in interpreting the final solution as the limit $\delta=0$ (Refs. 7, 8, and 13). Figure 2 shows the typical behavior of the eigenvalues $\lambda^{\pm}_{m,2n}$ as δ varies between $\delta=0$ and $\delta=\pi/2$ for Eversman's example[24] with $M=0.5$, $K_\infty=2$, and $\beta=0.72+i0.42$. We see that the eigenvalue corresponding to the exponentially increasing instability mode (designated by a star subsequently) changes to the other half-plane with increasing δ. Physically, this means that if the damping is sufficiently high, even the instability wave will decay rather than grow. Hence, for δ close to $\pi/2$, i.e., K almost imaginary, the correct multiplicative splitting is

$$\hat{\mathfrak{L}}^{(s)}(\xi;M)_{\oplus}=\mathfrak{L}^{(s)}(0)\prod_{n=0}^{\infty}\frac{1+\xi/\lambda^{-}_{m,2n}}{1+\xi/\gamma_{m,2n}} \tag{26a}$$

$$\hat{\mathfrak{L}}^{(s)}(\xi;M)_{\ominus}=\left(1-\frac{\xi}{\lambda^{+}_{m,-2}}\right)\left(1+\frac{\xi}{\lambda^{*}_{m}}\right)\prod_{n=0}^{\infty}\frac{1-\xi/\lambda^{+}_{m,2n}}{1-\xi/\gamma_{m,2n}} \tag{26b}$$

Here the remaining zeros in $\hat{\mathfrak{L}}^{(s)}_{\oplus}$ are reordered, now starting with $n=0$. In Eversman's example of Fig. 2 $\lambda^{*}_{m}\equiv\lambda^{-}_{m,0}$. The asymptotic behavior corresponding to Eqs. (25a) and (25b) is now

$$\hat{\mathfrak{L}}^{(s)}(\xi;M)_{\oplus}\sim\xi^{-1/2}\quad\text{as}\quad|\xi|\to\infty\ \text{in the}\ \oplus\ \text{plane} \tag{27a}$$

$$\hat{\mathfrak{L}}^{(s)}(\xi;M)_{\ominus}\sim\xi^{3/2}\quad\text{as}\quad|\xi|\to\infty\ \text{in the}\ \ominus\ \text{plane} \tag{27b}$$

The solution corresponding to the preceding splitting for complex K with δ close to $\pi/2$ automatically accounts for instability waves and usually is termed the "causal" solution. However, as pointed out by Crighton and Leppington[13] and Rienstra[8] for related semi-infinite problems, the unstable solution can also be obtained from the stable solution by adding the appropriate multiple of the unstable eigensolution. In the following we use both Eqs. (24) and (26).

Additive Decomposition—Edge Conditions

Proceeding with the formal solution of the generalized Wiener-Hopf equation (21) in the usual manner (e.g., Ref. 21), Eq. (21) is interpreted as a superposition of two ordinary semi-infinite Wiener-Hopf problems centered around the discontinuities in the boundary condition. First, we focus on the upstream discontinuity at $x=0$ and divide Eq. (21) by $\mathfrak{L}^{(s)}_{\oplus}$ where for the moment $\mathfrak{L}^{(s)}_{\oplus,\ominus}$ may denote either Eqs. (24) or (26)

$$\frac{\bar{g}^{(s)}_{\oplus}}{\mathfrak{L}^{(s)}_{\oplus}}-\frac{\mathfrak{L}^{(s)}_{\ominus}}{\mathfrak{L}^{(s)}_{\oplus}}\bar{\eta}^{(s)}_{m}+e^{-i\xi l}\frac{\bar{g}^{(s)}_{\ominus}}{\mathfrak{L}^{(s)}_{\oplus}}=\frac{1}{\mathfrak{L}^{(s)}_{\oplus}}\frac{\beta M}{1-M^2}\{\bar{R}^{(s)}_{m}-e^{-i\xi l}\bar{T}^{(s)}_{m}\}$$

$$+\frac{1}{\mathfrak{L}^{(s)}_{\oplus}}\frac{\beta M(1+M\xi/K)}{(1-M^2)^{3/2}}\frac{\cos(\tilde{\gamma}h/2)}{\tilde{\gamma}\sin(\tilde{\gamma}h/2)}\{\eta^{(s)}_{m}(0)-e^{-i\xi l}\eta^{(s)}_{m}(l)\}$$

Using the definition for $\mathfrak{L}^{(s)}$ to write

$$\frac{\cos(\tilde{\gamma}h/2)}{\tilde{\gamma}\sin(\tilde{\gamma}h/2)}=\frac{1-\mathfrak{L}^{(s)}(\xi)}{i\beta K\sqrt{1-M^2}\{(1+M\xi/K)/(1-M^2)\}^2} \tag{28}$$

the last term in the preceding equation can be expressed as

$$\eta^{(s)}_{m}(0)\frac{1-\mathfrak{L}^{(s)}(\xi)}{i(\xi+K/M)\mathfrak{L}^{(s)}_{\oplus}}$$

$$-\eta^{(s)}_{m}(l)e^{-i\xi l}\frac{\beta M(1+M\xi/K)\cos(\tilde{\gamma}h/2)}{\mathfrak{L}^{(s)}_{\oplus}(1-M^2)^{3/2}\tilde{\gamma}\sin(\tilde{\gamma}h/2)}$$

Then, the second step in the Wiener-Hopf solution procedure is the additive decomposition of all terms into two parts, one of which is holomorphic in an upper half-plane while the other is holomorphic in a lower half-plane. Formally this can always be achieved by means of the decomposition theorem (e.g., Ref. 21, p. 13) but often the decomposition can be found by mere inspection. Applying the decomposition theorem in the strip $-\mathrm{Min}\{\mathrm{Im}(\lambda^{-}_{m,2n})\}<-d<\mathrm{Im}\,\xi<-c<0$ we may write

$$e^{-i\xi l}\frac{\bar{g}^{(s)}_{\ominus}}{\mathfrak{L}^{(s)}_{\oplus}}=\bar{U}_{1\oplus}^{(s)}(\xi)+\bar{U}_{1\ominus}^{(s)}(\xi),$$

$$\bar{U}_{1\oplus}^{(s)}(\xi)=\frac{1}{2\pi i}\int_{-\infty-id}^{\infty-id}\frac{e^{-izl}\bar{g}^{(s)}_{\ominus}(z)}{(z-\xi)\mathfrak{L}^{(s)}_{\oplus}(z)}\,dz$$

$$\frac{\bar{R}^{(s)}_{m}}{\mathfrak{L}^{(s)}_{\oplus}}=\bar{S}_{1\oplus}^{(s)}(\xi)+\bar{S}_{1\ominus}^{(s)}(\xi),$$

$$\bar{S}_{1\ominus}^{(s)}(\xi)=\frac{(1+\gamma_{m,2s}M/K)\hat{\bar{E}}_{m,2s}}{i(\xi-\gamma_{m,2s})\mathfrak{L}^{(s)}_{\oplus}(\gamma_{m,2s})}$$

$$e^{-i\xi l}\frac{\bar{T}^{(s)}_{m}}{\mathfrak{L}^{(s)}_{\oplus}}=\bar{T}_{2\oplus}^{(s)}(\xi)+\bar{T}_{2\ominus}^{(s)}(\xi),$$

$$\bar{T}_{2\oplus}^{(s)}(\xi)=\frac{1}{2\pi i}\int_{-\infty-id}^{\infty-id}\frac{e^{-izl}\bar{T}^{(s)}_{m}(z)}{(z-\xi)\mathfrak{L}^{(s)}_{\oplus}(z)}\,dz$$

$$\frac{1}{i(\xi+K/M)\mathfrak{L}^{(s)}_{\oplus}}=\bar{V}_{1\oplus}^{(s)}(\xi)+\bar{V}_{1\ominus}^{(s)}(\xi),$$

$$\bar{V}_{1\ominus}^{(s)}(\xi)=\frac{1}{i(\xi+K/M)\mathfrak{L}^{(s)}_{\oplus}(-K/M)}$$

$$e^{-i\xi l}\frac{\beta M(1+M\xi/K)\cos(\tilde{\gamma}h/2)}{\mathfrak{L}^{(s)}_{\oplus}(1-M^2)^{3/2}\tilde{\gamma}\sin(\tilde{\gamma}h/2)}=\bar{W}_{2\oplus}^{(s)}(\xi)+\bar{W}_{2\ominus}^{(s)}(\xi),$$

$$\bar{W}_{2\oplus}^{(s)}(\xi)=\frac{\beta M}{(1-M^2)^{3/2}}$$

$$\times\frac{1}{2\pi i}\int_{-\infty-id}^{\infty-id}\frac{e^{-izl}(1+Mz/K)\cos(\tilde{\gamma}h/2)}{(z-\xi)\mathfrak{L}^{(s)}_{\oplus}(z)\tilde{\gamma}\sin(\tilde{\gamma}h/2)}\,dz$$

Now collecting all terms holomorphic in $\mathrm{Im}\,\xi>-\mathrm{Min}\{\mathrm{Im}(\lambda^{-}_{m,2n})\}$ on the left-hand side and all terms holomorphic in $\mathrm{Im}\,\xi<0$ on the right-hand side we find

$$\frac{\bar{g}^{(s)}_{\oplus}}{\mathfrak{L}^{(s)}_{\oplus}}+\bar{U}_{1\oplus}^{(s)}-\frac{\beta M}{1-M^2}(\bar{S}_{1\oplus}^{(s)}-\bar{T}_{2\oplus}^{(s)})-\eta^{(s)}_{m}(0)\bar{V}_{1\oplus}^{(s)}$$

$$+\eta^{(s)}_{m}(l)\bar{W}_{2\oplus}^{(s)}=\mathfrak{L}^{(s)}_{\ominus}\bar{\eta}^{(s)}_{m}-\bar{U}_{1\ominus}^{(s)}+\frac{\beta M}{1-M^2}(\bar{S}_{1\ominus}^{(s)}-\bar{T}_{2\ominus}^{(s)})$$

$$+\eta^{(s)}_{m}(0)\left[\bar{V}_{1\ominus}^{(s)}-\frac{\mathfrak{L}^{(s)}_{\ominus}}{i(\xi+K/M)}\right]-\eta^{(s)}_{m}(l)\bar{W}_{2\ominus}^{(s)}\equiv J_1(\xi) \tag{29}$$

Due to the overlap of the upper and lower half-plane of holomorphy the two sides are analytic continuations of one and the same holomorphic function $J_1(\xi)$ defined in the whole complex ξ plane. That this is also true for generalized functions is asserted by the "edge of the wedge theorem."[33] Using Liouville's theorem the function $J_1(\xi)$ is determined from the asymptotic behavior of the involved functions for large ξ in the respective half-plane. This asymptotic behavior is governed by the edge conditions. Postponing the actual specification of the edge condition at $x=0$ until later, we choose the generally least singular solution by setting $J_1(\xi)$

identically equal to zero such that

$$\bar{g}_{\oplus}^{(s)} = -\mathcal{L}_{\oplus}^{(s)}\left\{\bar{U}_{1\oplus}^{(s)} - \frac{\beta M}{1-M^2}(\bar{S}_{1\oplus}^{(s)} - \bar{T}_{2\oplus}^{(s)}) - \eta_m^{(s)}(0)\,\bar{V}_{1\oplus}^{(s)} + \eta_m^{(s)}(l)\,\bar{W}_{2\oplus}^{(s)}\right\} \tag{30a}$$

$$\bar{\eta}_m^{(s)} = \frac{1}{\mathcal{L}_{\ominus}^{(s)}}\left\{\bar{U}_{1\ominus}^{(s)} - \frac{\beta M}{1-M^2}(\bar{S}_{1\ominus}^{(s)} - \bar{T}_{2\ominus}^{(s)}) - \eta_m^{(s)}(0)\left[\bar{V}_{1\ominus}^{(s)} - \frac{\mathcal{L}_{\ominus}^{(s)}}{i(\xi+K/M)}\right] + \eta_m^{(s)}(l)\,\bar{W}_{2\ominus}^{(s)}\right\} \tag{30b}$$

Aside from the different factorizations [Eqs. (24) and (26)] we still have the unknown jumps $\eta_m^{(s)}(0)$ and $\eta_m^{(s)}(l)$ at our disposal to enforce certain edge conditions.

Proceeding now similarly with the treatment of the downstream discontinuity of the boundary condition at $x=l$, we multiply Eq. (21) by $\exp(i\xi l)/\mathcal{L}_{\ominus}^{(s)}$ and again use Eq. (28) to find

$$e^{i\xi l}\frac{\bar{g}_{\oplus}^{(s)}}{\mathcal{L}_{\ominus}^{(s)}} - e^{i\xi l}\mathcal{L}_{\oplus}^{(s)}\bar{\eta}_m^{(s)} + \frac{\bar{g}_{\ominus}^{(s)}}{\mathcal{L}_{\ominus}^{(s)}} = \frac{e^{i\xi l}}{\mathcal{L}_{\ominus}^{(s)}}\frac{\beta M}{1-M^2}\{\bar{R}_m^{(s)} - e^{-i\xi l}\bar{T}_m^{(s)}\} + e^{i\xi l}\eta_m^{(s)}(0)\frac{\beta M(1+M\xi/K)\cos(\tilde{\gamma}h/2)}{\mathcal{L}_{\ominus}^{(s)}(1-M^2)^{3/2}\tilde{\gamma}\sin(\tilde{\gamma}h/2)} - \eta_m^{(s)}(l)\frac{1-\mathcal{L}^{(s)}(\xi)}{i(\xi+K/M)\mathcal{L}_{\ominus}^{(s)}}$$

Now, the additive decomposition has to be performed in the strip $0<f<\mathrm{Im}\,\xi<e<\mathrm{Min}\{\mathrm{Im}(\lambda_{m,2n}^{+})\}$. We write

$$e^{i\xi l}\frac{\bar{g}_{\oplus}^{(s)}}{\mathcal{L}_{\ominus}^{(s)}} = \bar{U}_{2\oplus}^{(s)}(\xi) + \bar{U}_{2\ominus}^{(s)}(\xi),$$

$$\bar{U}_{2\ominus}^{(s)}(\xi) = -\frac{1}{2\pi i}\int_{-\infty+ie}^{\infty+ie}\frac{e^{izl}\bar{g}_{\oplus}^{(s)}(z)}{(z-\xi)\mathcal{L}_{\ominus}^{(s)}(z)}\,dz$$

$$e^{i\xi l}\frac{\bar{R}_m^{(s)}}{\mathcal{L}_{\ominus}^{(s)}} = \bar{S}_{2\oplus}^{(s)}(\xi) + \bar{S}_{2\ominus}^{(s)}(\xi),$$

$$\bar{S}_{2\ominus}^{(s)}(\xi) = -\frac{1}{2\pi i}\int_{-\infty+ie}^{\infty+ie}\frac{e^{izl}\bar{R}_m^{(s)}}{(z-\xi)\mathcal{L}_{\ominus}^{(s)}(z)}\,dz$$

$$\frac{\bar{T}_m^{(s)}}{\mathcal{L}_{\ominus}^{(s)}} = \bar{T}_{1\oplus}^{(s)}(\xi) + \bar{T}_{1\ominus}^{(s)}(\xi),$$

$$\bar{T}_{1\oplus}^{(s)}(\xi) = \frac{(1-\gamma_{m,2s}M/K)e^{-i\gamma_{m,2s}l}\hat{\bar{E}}_{m,2s}}{i(\xi+\gamma_{m,2s})\mathcal{L}_{\ominus}^{(s)}(-\gamma_{m,2s})}$$

$$\frac{1}{i(\xi+K/M)\mathcal{L}_{\ominus}^{(s)}} = \bar{W}_{1\oplus}^{(s)}(\xi) + \bar{W}_{1\ominus}^{(s)}(\xi),$$

$$\bar{W}_{1\oplus}^{(s)}(\xi) = \frac{1}{i(\xi+K/M)\mathcal{L}_{\ominus}^{(s)}(-K/M)}$$

$$e^{i\xi l}\frac{\beta M(1+M\xi/K)\cos(\tilde{\gamma}h/2)}{\mathcal{L}_{\ominus}^{(s)}(1-M^2)^{3/2}\tilde{\gamma}\sin(\tilde{\gamma}h/2)} = \bar{V}_{2\oplus}^{(s)}(\xi) + \bar{V}_{2\ominus}^{(s)}(\xi),$$

$$\bar{V}_{2\ominus}^{(s)}(\xi) = -\frac{\beta M}{(1-M^2)^{3/2}} \times \frac{1}{2\pi i}\int_{-\infty+ie}^{\infty+ie}\frac{e^{izl}(1+Mz/K)\cos(\tilde{\gamma}h/2)}{(z-\xi)\mathcal{L}_{\ominus}^{(s)}(z)\tilde{\gamma}\sin(\tilde{\gamma}h/2)}\,dz$$

such that after collecting all terms holomorphic in $\mathrm{Im}\,\xi>0$ on the left-hand side and all terms holomorphic in $\mathrm{Im}\,\xi<\mathrm{Min}\{\mathrm{Im}(\lambda_{m,2n}^{+})\}$ on the right-hand side

$$\bar{U}_{2\oplus}^{(s)} - e^{i\xi l}\bar{\eta}_m^{(s)}\mathcal{L}_{\oplus}^{(s)} - \frac{\beta M}{1-M^2}(\bar{S}_{2\oplus}^{(s)} - \bar{T}_{1\oplus}^{(s)}) - \eta_m^{(s)}(0)\,\bar{V}_{2\oplus}^{(s)} + \eta_m^{(s)}(l)\left[\bar{W}_{1\oplus}^{(s)} - \frac{\mathcal{L}_{\oplus}^{(s)}}{i(\xi+K/M)}\right] = -\frac{\bar{g}_{\ominus}^{(s)}}{\mathcal{L}_{\ominus}^{(s)}} - \bar{U}_{2\ominus}^{(s)} + \frac{\beta M}{1-M^2} \times (\bar{S}_{2\ominus}^{(s)} - \bar{T}_{1\ominus}^{(s)}) + \eta_m^{(s)}(0)\,\bar{V}_{2\ominus}^{(s)} - \eta_m^{(s)}(l)\,\bar{W}_{1\ominus}^{(s)} \equiv J_2(\xi) \tag{31}$$

Again we postpone the specification of the edge condition and choose $J_2(\xi)\equiv 0$

$$e^{i\xi l}\bar{\eta}_m^{(s)} = \frac{1}{\mathcal{L}_{\oplus}^{(s)}}\left\{\bar{U}_{2\oplus}^{(s)} - \frac{\beta M}{1-M^2}(\bar{S}_{2\oplus}^{(s)} - \bar{T}_{1\oplus}^{(s)}) - \eta_m^{(s)}(0)\,\bar{V}_{2\oplus}^{(s)} + \eta_m^{(s)}(l)\left[\bar{W}_{1\oplus}^{(s)} - \frac{\mathcal{L}_{\oplus}^{(s)}}{i(\xi+K/M)}\right]\right\} \tag{32a}$$

$$\bar{g}_{\ominus}^{(s)} = \mathcal{L}_{\ominus}^{(s)}\left\{-\bar{U}_{2\ominus}^{(s)} + \frac{\beta M}{1-M^2}(\bar{S}_{2\ominus}^{(s)} - \bar{T}_{1\ominus}^{(s)}) + \eta_m^{(s)}(0)\,\bar{V}_{2\ominus}^{(s)} - \eta_m^{(s)}(l)\,\bar{W}_{1\ominus}^{(s)}\right\} \tag{32b}$$

For the following it is advantageous to introduce the two new unknown functions

$$\bar{u}_{\ominus}^{(s)^*}(\xi) = \left\{\bar{g}_{\ominus}^{(s)} + \frac{\beta M}{1-M^2}\bar{T}_m^{(s)}\right\}\Big/\mathcal{L}_{\ominus}^{(s)} \tag{33a}$$

$$\bar{u}_{\oplus}^{(s)^*}(\xi) = \left\{\bar{g}_{\oplus}^{(s)} - \frac{\beta M}{1-M^2}\bar{R}_m^{(s)}\right\}\Big/\mathcal{L}_{\oplus}^{(s)} \tag{33b}$$

where $\bar{u}_{\ominus}^{(s)^*}$ is holomorphic in the lower half-plane $\mathrm{Im}\,\xi<\mathrm{Min}\{\mathrm{Im}(\lambda_{m,2n}^{+})\}$ with the exception of a pole at $\xi=-\gamma_{m,2s}$ and $\bar{u}_{\oplus}^{(s)^*}$ is holomorphic in the upper half-plane $\mathrm{Im}\,\xi>-\mathrm{Min}\{\mathrm{Im}(\lambda_{m,2n}^{-})\}$ with the exception of a pole at $\xi=\gamma_{m,2s}$. Then the decomposition integrals for the $\oplus$ functions of Eq. (29) can be evaluated by closing the integration contour in the lower half-plane. Applying the residue theorem we find

$$\bar{U}_{1\oplus}^{(s)} + \frac{\beta M}{1-M^2}\bar{T}_{2\oplus}^{(s)} = \sum_{n=-1}^{\infty}\frac{P_{2n}^{(s)}(-\lambda_{m,2n}^{-})}{\xi+\lambda_{m,2n}^{-}}\bar{u}_{\ominus}^{(s)^*}(-\lambda_{m,2n}^{-})$$

$$\bar{W}_{2\oplus}^{(s)} = \sum_{n=-1}^{\infty}\frac{R_{2n}^{(s)}(-\lambda_{m,2n}^{-})}{\xi+\lambda_{m,2n}^{-}}$$

where

$$P_{2n}^{(s)}(-\lambda_{m,2n}^{-}) = \{\exp(i\lambda_{m,2n}^{-}l)[\mathcal{L}_{\ominus}^{(s)}(-\lambda_{m,2n}^{-})]^2\lambda_{2n}^{-2}\} \div \left\{\lambda_{m,2n}^{-}\left[1 + \frac{i\beta Kh}{2}\sqrt{1-M^2}\left\{\frac{1-\lambda_{m,2n}^{-}M/K}{1-M^2}\right\}^2 + \frac{h\lambda_{2n}^{-2}}{2i\beta K\sqrt{1-M^2}}\left\{\frac{1-M^2}{1-\lambda_{m,2n}^{-}M/K}\right\}^2\right] - \frac{2\lambda_{2n}^{-2}M/K}{1-\lambda_{m,2n}^{-}M/K}\right\}$$

$$R_{2n}^{(s)}(-\lambda_{m,2n}^{-}) = \frac{M}{iK}\frac{P_{2n}^{(s)}(-\lambda_{m,2n}^{-})}{\mathcal{L}_{\ominus}^{(s)}(-\lambda_{m,2n}^{-})\{1-\lambda_{m,2n}^{-}M/K\}}$$

Similarly, the decomposition integrals for the $\ominus$ functions of Eq. (31) can be evaluated by closing the integration contour

in the upper half-plane such that

$$\bar{U}_{2_{\ominus}}^{(s)} - \frac{\beta M}{1-M^2}\bar{S}_{2_{\ominus}}^{(s)} = \sum_{n=-1}^{\infty} \frac{Q_{2n}^{(s)}(\lambda_{m,2n}^{+})}{\xi-\lambda_{m,2n}^{+}}\bar{u}_{\oplus}^{(s)*}(\lambda_{m,2n}^{+})$$

$$\bar{V}_{2_{\ominus}}^{(s)} = \sum_{n=-1}^{\infty} \frac{S_{2n}^{(s)}(\lambda_{m,2n}^{+})}{\xi-\lambda_{m,2n}^{+}}$$

with

$$Q_{2n}^{(s)}(\lambda_{m,2n}^{+}) = \{-\exp(i\lambda_{m,2n}^{+}l)[\mathfrak{L}_{\oplus}^{(s)}(\lambda_{m,2n}^{+})]^2\lambda_{2}^{+2}{}_{n}\}$$
$$\div\left\{\lambda_{m,2n}^{+}\left[1+\frac{i\beta Kh}{2}\sqrt{1-M^2}\left\{\frac{1+\lambda_{m,2n}^{+}M/K}{1-M^2}\right\}^2\right.\right.$$
$$\left.\left.+\frac{h\lambda_{2}^{+2}{}_{n}}{2i\beta K\sqrt{1-M^2}}\left\{\frac{1-M^2}{1+\lambda_{m,2n}^{+}M/K}\right\}^2\right]+\frac{2\lambda_{2}^{+2}{}_{n}M/K}{1+\lambda_{m,2n}^{+}M/K}\right\}$$

$$S_{2n}^{(s)}(\lambda_{m,2n}^{+}) = \frac{M}{iK}\frac{Q_{2n}^{(s)}(\lambda_{m,2n}^{+})}{\mathfrak{L}_{\oplus}^{(s)}(\lambda_{m,2n}^{+})\{1+\lambda_{m,2n}^{+}M/K\}}$$

In obtaining this series the conventional kernel splitting Eqs. (24) were used. Exactly analogous formulas are found by using Eqs. (26) instead of Eqs. (24) if only λ_{m}^{*} is counted as belonging to the zeros $\lambda_{m,2n}^{+}$.

If we substitute the preceding results, the left-hand side of Eq. (29) and the right-hand side of Eq. (31) can be written in the form

$$\bar{u}_{\oplus}^{(s)*}(\xi) + \sum_{n=-1}^{\infty}\frac{P_{2n}^{(s)}(-\lambda_{m,2n}^{-})}{\xi+\lambda_{m,2n}^{-}}\bar{u}_{\ominus}^{(s)*}(-\lambda_{m,2n}^{-})$$
$$= \frac{-\beta M}{1-M^2}\frac{(1+\gamma_{m,2s}M/K)\hat{\bar{E}}_{m,2s}}{i(\xi-\gamma_{m,2s})\mathfrak{L}_{\oplus}^{(s)}(\gamma_{m,2s})}$$
$$+\eta_{m}^{(s)}(0)\frac{1}{i(\xi+K/M)}\left\{\frac{1}{\mathfrak{L}_{\oplus}^{(s)}(\xi)}-\frac{1}{\mathfrak{L}_{\oplus}^{(s)}(-K/M)}\right\}$$
$$-\eta_{m}^{(s)}(l)\sum_{n=-1}^{\infty}\frac{R_{2n}^{(s)}(-\lambda_{m,2n}^{-})}{\xi+\lambda_{m,2n}^{-}} \tag{34}$$

$$\bar{u}_{\ominus}^{(s)*}(\xi) + \sum_{n=-1}^{\infty}\frac{Q_{2n}^{(s)}(\lambda_{m,2n}^{+})}{\xi-\lambda_{m,2n}^{+}}\bar{u}_{\oplus}^{(s)*}(\lambda_{m,2n}^{+})$$
$$= \frac{\beta M}{1-M^2}\frac{(1-\gamma_{m,2s}M/K)e^{-i\gamma_{m,2s}l}\hat{\bar{E}}_{m,2s}}{i(\xi+\gamma_{m,2s})\mathfrak{L}_{\ominus}^{(s)}(-\gamma_{m,2s})}$$
$$+\eta_{m}^{(s)}(0)\sum_{n=-1}^{\infty}\frac{S_{2n}^{(s)}(\lambda_{m,2n}^{+})}{\xi-\lambda_{m,2n}^{+}}$$
$$-\eta_{m}^{(s)}(l)\frac{1}{i(\xi+K/M)}\left\{\frac{1}{\mathfrak{L}_{\ominus}^{(s)}(\xi)}-\frac{1}{\mathfrak{L}_{\ominus}^{(s)}(-K/M)}\right\} \tag{35}$$

Before proceeding with the solution we have to specify the displacement jumps $\eta_{m}^{(s)}(0)$ and $\eta_{m}^{(s)}(l)$, i.e., we have to resume the discussion of the *edge conditions*. As an indication of the mathematical nonuniqueness of the solution there are several possible edge conditions which are best studied by evaluating Eqs. (30) and (32) asymptotically for large $|\xi|$ and applying the Abelian theorems (cf. Ref. 21, p. 36). First, we consider the conventional factorization, Eqs. (24). Making use of Eqs. (25) and the various residue evaluations we distinguish the following main cases.

A. $\eta_{m}^{(s)}(0) = \eta_{m}^{(s)}(l) \equiv 0$

Then for $|\xi| \to \infty$ we find

$$\bar{g}_{\oplus}^{(s)} \sim \xi^{-1/2} \to g_{-}^{(s)}(x) \sim x^{-1/2} \text{ as } x \to 0^{-}$$

$$\bar{\eta}_{m}^{(s)} \sim \xi^{-3/2} \to \eta_{m}^{(s)}(x) \sim x^{1/2} \text{ as } x \to 0^{+}$$

$$e^{i\xi l}\bar{\eta}_{m}^{(s)} \sim \xi^{-3/2} \to \eta_{m}^{(s)}(x) \sim (x-l)^{1/2} \text{ as } x \to l^{-}$$

$$\bar{g}_{\ominus}^{(s)} \sim \xi^{-1/2} \to g_{+}^{(s)}(x) \sim (x-l)^{-1/2} \text{ as } x \to l^{+}$$

The edge conditions just given were assumed for the *singularity solution* of Namba and Fukushige.[25]

B. $\eta_{m}^{(s)}(0)$ and $\eta_{m}^{(s)}(l)$ Finite

One way of explicitly determining these finite jumps is to choose them such that the pressure remains finite at $x=0$, l, i.e., all $\xi^{-1/2}$ terms in $\bar{g}_{\oplus}^{(s)}$ and $\bar{g}_{\ominus}^{(s)}$ have to vanish for $|\xi|$ large

$$\eta_{m}^{(s)}(0)\frac{1}{i\mathfrak{L}_{\oplus}^{(s)}(-K/M)} + \eta_{m}^{(s)}(l)\sum_{n=-1}^{\infty}R_{2n}^{(s)}(-\lambda_{m,2n}^{-})$$
$$= -\frac{\beta M}{1-M^2}\frac{(1+\gamma_{m,2s}M/K)\hat{\bar{E}}_{m,2s}}{i\mathfrak{L}_{\oplus}^{(s)}(\gamma_{m,2s})}$$
$$-\sum_{n=-1}^{\infty}P_{2n}^{(s)}(-\lambda_{m,2n}^{-})\bar{u}_{\ominus}^{(s)*}(-\lambda_{m,2n}^{-})$$

$$\eta_{m}^{(s)}(0)\sum_{n=-1}^{\infty}S_{2n}^{(s)}(\lambda_{m,2n}^{+}) + \eta_{m}^{(s)}(l)\frac{1}{i\mathfrak{L}_{\ominus}^{(s)}(-K/M)}$$
$$= -\frac{\beta M}{1-M^2}\frac{(1-\gamma_{m,2s}M/K)e^{-i\gamma_{m,2s}l}\hat{\bar{E}}_{m,2s}}{i\mathfrak{L}_{\ominus}^{(s)}(-\gamma_{m,2s})}$$
$$+\sum_{n=-1}^{\infty}Q_{2n}^{(s)}(\lambda_{m,2n}^{+})\bar{u}_{\oplus}^{(s)*}(\lambda_{m,2n}^{+})$$

The result corresponding to this assumption appears to be identical to the *mode matching solution* (cf. Ref. 26) which implicitly assumes continuous changes in M starting with the $M=0$ case where displacement jumps occur at $x=0$, l (cf. Ref. 23 and see, also, Fig. 8).

C. $\eta_{m}^{(s)}(0) = 0$ and $\eta_{m}^{(s)}(l)$ Finite

In this case one can choose $\eta_{m}^{(s)}(l)$ such that the Kutta condition is satisfied at $x=0$, i.e., all $\xi^{-3/2}$ terms in $\bar{\eta}_{m}^{(s)}$ have to vanish for large $|\xi|$

$$\eta_{m}^{(s)}(l) = \frac{-1}{\sum_{n=-1}^{\infty}R_{2n}^{(s)}(-\lambda_{m,2n}^{-})}\left\{\frac{\beta M}{1-M^2}\frac{(1+\gamma_{m,2s}M/K)\hat{\bar{E}}_{m,2s}}{i\mathfrak{L}_{\oplus}^{(s)}(\gamma_{m,2s})}\right.$$
$$\left.+\sum_{n=-1}^{\infty}P_{2n}^{(s)}(-\lambda_{m,2n}^{-})\bar{u}_{\ominus}^{(s)*}(-\lambda_{m,2n}^{-})\right\}$$

The pressure remains finite at $x=0$, l. We are not aware of any solutions for the liner problem which exhibit this behavior but the finite vortex sheet solution of Crighton and Innes[27] appears to fall into this category.

Switching now to the "causal" factorization, Eqs. (26) and admitting an infinite displacement jump at $x=l$ the following solution is obtained.

D. $\eta_{m}^{(s)}(0) = 0$, $d\eta_{m}^{(s)}/dx(0) = 0$, $\eta_{m}^{(s)}(l)$ Infinite

$$\bar{g}_{\oplus}^{(s)} \sim \xi^{-3/2} \to g_{-}^{(s)}(x) \sim x^{1/2} \text{ as } x \to 0^{-}$$

$$\bar{\eta}_m^{(s)} \sim \xi^{-5/2} \to \eta(x) \sim x^{3/2} \text{ as } x \to 0^+$$

$$e^{i\xi l}\bar{\eta}_m^{(s)} \sim \xi^{-1/2} \to \eta(x) \sim (x-l)^{-1/2} \text{ as } x \to l^-$$

$$\bar{g}_{\ominus}^{(s)} \sim \xi^{1/2} \to g_+^{(s)}(x) \sim (x-l)^{-3/2} \text{ as } x \to l^+$$

The Kutta condition is satisfied at $x=0$, however, the singular behavior near the trailing edge requires the inclusion of generalized functions. The preceding solution case D corresponds to the semi-infinite solutions of Nilsson and Brander[20] while for the finite vortex sheet problem Howe[28] studied a corresponding solution.

All preceding solutions differ by multiples of eigensolutions and the tantalizing question is which solution (if any) is the physically correct one. In general, this can only be answered by comparing the various solutions with careful experimental results.

Formal Solution— Reflection and Transmission Coefficients

Substituting the displacement jumps $\eta_m^{(s)}(0)$, $\eta_m^{(s)}(l)$ for the chosen edge conditions into Eqs. (34) and (35) these equations still contain the infinitely many unknown constants $\bar{u}_{\ominus}^{(s)*}(-\lambda_{m,2n}^-)$ and $\bar{u}_{\oplus}^{(s)*}(\lambda_{m,2n}^+)$, $n=-1,0,1\ldots$. Setting $\xi=\lambda_{m,2\sigma}^+$ in Eq. (34) and $\xi=-\lambda_{m,2\sigma}^-$ in Eq. (35) with $\sigma=-1,0,1\ldots$, an infinite system of algebraic determination equations is obtained for these unknown constants. This infinite system can be solved approximately by the *method of truncation*. Since the expressions for $P_{2n}^{(s)}$ and $Q_{2n}^{(s)}$ contain exponential terms of the form $\exp(i\lambda_{m,2n}^{\pm}l)$, in general, very few terms need to be kept in order to obtain already rather accurate approximate solutions as long as l/h is not too small and hK is not too large.

Once the unknown constants $\bar{u}_{\ominus}^{(s)*}(-\lambda_{m,2n}^-)$ and $\bar{u}_{\oplus}^{(s)*}(\lambda_{m,2n}^+)$, $n=-1,0,1,\ldots$, are determined, the solution φ_m can be found in the whole field as follows. From Eq. (30b) [or equivalently, Eq. (32a)] together with the definitions Eqs. (33a) and (33b) and using Eq. (34) we find

$$\bar{\eta}_m^{(s)}(\xi) = \frac{\exp(-i\xi l)\,\bar{u}_{\ominus}^{(s)*}(\xi)}{\mathcal{L}_{\oplus}^{(s)}(\xi)} + \frac{\bar{u}_{\oplus}^{(s)*}(\xi)}{\mathcal{L}_{\ominus}^{(s)}(\xi)} - \frac{\beta M}{(1-M^2)^{3/2}} \times \frac{(1+\xi M/K)\cos(\tilde{\gamma}h/2)}{\tilde{\gamma}\sin(\tilde{\gamma}h/2)\,\mathcal{L}^{(s)}(\xi)}\left[\eta_m^{(s)}(0) - e^{-i\xi l}\eta_m^{(s)}(l)\right] \tag{36}$$

Observing the definition $\bar{\eta}_m^{(s)} = \bar{\eta}_m^{(o)} = -\bar{\eta}_m^{(i)}$ for symmetric excitation the preceding solution for $\bar{\eta}_m^{(s)}$ may be substituted into Eq. (20) which, upon Fourier inversion, gives φ_m in the whole field.

In addition, all we need to determine are the unknown amplitudes $\bar{R}_{m,2n}$ and $\bar{T}_{m,2n}$ of the cut-on reflected and transmitted waves. These can be evaluated directly by observing that according to Eq. (33b) $\bar{g}_{\oplus}^{(s)}$ is holomorphic in the upper half-plane, as postulated in Eq. (19a), only if the residues at $\xi=-\gamma_{m,2\sigma}$, $\sigma=0,1,\ldots,N^{(s)}$ vanish, i.e.,

$$\hat{\bar{R}}_{m,2\sigma} = \frac{-i(1-M^2)\,\bar{u}_{\oplus}^{(s)*}(-\gamma_{m,2\sigma})}{\beta M(1-\gamma_{m,2\sigma}M/K)} \times \lim_{\xi\to-\gamma_{m,2\sigma}}\{(\xi+\gamma_{m,2\sigma})\,\mathcal{L}_{\oplus}^{(s)}(\xi)\}$$

Substituting Eq. (23) for $\mathcal{L}_{\oplus}^{(s)}$ and using l'Hospital's rule we find after inserting Eq. (34) with $\xi=-\gamma_{m,2\sigma}$ for $\bar{u}_{\oplus}^{(s)*}(-\gamma_{m,2\sigma})$

$$\hat{\bar{R}}_{m,2\sigma} = \frac{-2K(1-\gamma_{m,2\sigma}M/K)}{Mh\sqrt{1-M^2}\gamma_{m,2\sigma}(1+\delta_{\sigma,0})\,\mathcal{L}_{\ominus}^{(s)}(-\gamma_{m,2\sigma})} \times \left\{\frac{\beta M}{1-M^2}\,\frac{(1+\gamma_{m,2s}M/K)\,\hat{\bar{E}}_{m,2s}}{i(\gamma_{m,2\sigma}+\gamma_{m,2s})\,\mathcal{L}_{\oplus}^{(s)}(\gamma_{m,2s})} + \sum_{n=-1}^{\infty}\frac{P_{2n}^{(s)}(-\lambda_{m,2n}^-)}{\gamma_{m,2\sigma}-\lambda_{m,2n}^-}\,\bar{u}_{\ominus}^{(s)*}(-\lambda_{m,2n}^-) + \eta_m^{(s)}(0)\,\frac{1}{i(\gamma_{m,2\sigma}-K/M)\,\mathcal{L}_{\oplus}^{(s)}(-K/M)} + \eta_m^{(s)}(l) \times \sum_{n=-1}^{\infty}\frac{R_{2n}^{(s)}(-\lambda_{m,2n}^-)}{\gamma_{m,2\sigma}-\lambda_{m,2n}^-}\right\}, \quad \sigma=0,1,\ldots,N^{(s)} \tag{37}$$

Similarly, using definition (33a), we find

$$\hat{\bar{T}}_{m,2\sigma} = \frac{e^{-i\gamma_{m,2\sigma}l}\,i(1-M^2)\,\bar{u}_{\ominus}^{(s)*}(\gamma_{m,2\sigma})}{\beta M(1+\gamma_{m,2\sigma}M/K)} \times \lim_{\xi\to\gamma_{m,2\sigma}}\{(\xi-\gamma_{m,2\sigma})\,\mathcal{L}_{\ominus}^{(s)}(\xi)\}$$

and, finally, after employing Eq. (35)

$$\hat{\bar{T}}_{m,2\sigma} = \frac{-2K\exp(-i\gamma_{m,2\sigma}l)\,(1+\gamma_{m,2\sigma}M/K)}{Mh\sqrt{1-M^2}\gamma_{m,2\sigma}(1+\delta_{\sigma,0})\,\mathcal{L}_{\oplus}^{(s)}(\gamma_{m,2\sigma})} \times \left\{\frac{\beta M}{1-M^2}\,\frac{(1-\gamma_{m,2s}M/K)\,e^{-i\gamma_{m,2s}l}\,\hat{\bar{E}}_{m,2s}}{i(\gamma_{m,2\sigma}+\gamma_{m,2s})\,\mathcal{L}_{\ominus}^{(s)}(-\gamma_{m,2s})} - \sum_{n=-1}^{\infty}\frac{Q_{2n}^{(s)}(\lambda_{m,2n}^+)}{\gamma_{m,2\sigma}-\lambda_{m,2n}^+}\,\bar{u}_{\oplus}^{(s)*}(\lambda_{m,2n}^+) + \eta_m^{(s)}(0)\sum_{n=-1}^{\infty}\frac{S_{2n}^{(s)}(\lambda_{m,2n}^+)}{\gamma_{m,2\sigma}-\lambda_{m,2n}^+} + \eta_m^{(s)}(l)\,\frac{1}{i(\gamma_{m,2\sigma}-K/M)\,\mathcal{L}_{\ominus}^{(s)}(-K/M)}\right\}, \quad \sigma=0,1,\ldots,N^{(s)} \tag{38}$$

It is to be noted that all amplitudes are defined with reference to $x=0$. For the applications it is more appropriate to define $\hat{\bar{E}}_{m,2s}$ and $\hat{\bar{T}}_{m,2\sigma}$ with respect to the exit plane $x=l$. Adding the corresponding phase factors we find

$$\hat{\bar{E}}_{m,2s}^* = e^{-i\gamma_{m,2s}l}\,\hat{\bar{E}}_{m,2s}, \qquad \hat{\bar{T}}_{m,2\sigma}^* = e^{i\gamma_{m,2\sigma}l}\,\hat{\bar{T}}_{m,2\sigma}$$

It can be shown that expressions (37) and (38) apply not only to the cut-on modes but also to the cut-off modes. Therefore, omitting φ_m in Eq. (11) and ψ_m in Eq. (12) and letting $N\to\infty$ there, we already have the solution for $\Phi_m(x,z)$ in the hard wall sections. Similarly, one may circumvene the Fourier inversion of $\bar{\varphi}_m$ for $0\le x\le l$ if we observe that the soft wall separation-of-variables solution $\Phi_m(x,z)$ will be of the form

$$\Phi_m(x,z) = \sum_{n=-1}^{\infty}\{\vec{\bar{C}}_{m,2n}e^{i\lambda_{m,2n}^+x}\tilde{\psi}_{2n}^+(z) + \overleftarrow{\bar{C}}_{m,2n}e^{i\lambda_{m,2n}^-(l-x)}\tilde{\psi}_{2n}^-(z)\} \tag{39}$$

where the transversal soft wall eigenfunctions are

$$\tilde{\psi}_{2n}^{\pm}(z) = \cos(\lambda_{2n}^{\pm}z) + \frac{iK_\infty\beta}{\lambda_{2n}^{\pm}}\left\{\frac{1\pm\lambda_{m,2n}^{\pm}M/K}{1-M^2}\right\}^2\sin(\lambda_{2n}^{\pm}z) \tag{40}$$

Fourier inverting Eq. (36) for $\eta_m^{(s)}(x)$ and substituting the preceding Φ_m into the boundary condition Eq. (9), the amplitudes $\vec{\bar{C}}_{m,2n}$ and $\overleftarrow{\bar{C}}_{m,2n}$ can be determined by comparing coefficients. The pressure is obtained in the whole field from Eq. (3).

In any modal approach the *reflection and transmission factors* are of prime importance. For upstream incidence these

are $\vec{r}_{m,2s;2\sigma} = \vec{R}_{m,2\sigma}/\vec{E}_{m,2s}$ and $\vec{t}_{m,2s;2\sigma} = \vec{T}^{*}_{m,2\sigma}/\vec{E}_{m,2s}$, while for downstream incidence they are given by $\overleftarrow{r}_{m,2s;2\sigma} = \overleftarrow{T}^{*}_{m,2\sigma}/\overleftarrow{E}^{*}_{m,2s}$ and $\overleftarrow{t}_{m,2s;2\sigma} = \overleftarrow{R}_{m,2\sigma}/\overleftarrow{E}^{*}_{m,2s}$ and can be obtained at once from Eqs. (37) and (38). The corresponding *reflection* and *transmission coefficients* $\rho_{m,2s;2\sigma}$ and $\tau_{m,2s;2\sigma}$ for the cut-on modes s, $\sigma = 0,1,\ldots,N^{(s)}$, defined as the ratios of the reflected or transmitted acoustic power in the $(m,2\sigma)$th mode to the acoustic power of the incoming $(m,2s)$th mode, are then for upstream incidence (i.e., $\vec{E}_{m,2s} = 0$)

$$\vec{\rho}_{m,2s;2\sigma} = \frac{\gamma_{m,2\sigma}}{\gamma_{m,2s}} \frac{2-\delta_{s,0}}{2-\delta_{\sigma,0}} |\vec{r}_{m,2s;2\sigma}|^2$$

$$\vec{\tau}_{m,2s;2\sigma} = \frac{\gamma_{m,2\sigma}}{\gamma_{m,2s}} \frac{2-\delta_{s,0}}{2-\delta_{\sigma,0}} |\vec{t}_{m,2s;2\sigma}|^2$$

and for the incidence from downstream (i.e., $\overleftarrow{E}_{m,2s} = 0$)

$$\overleftarrow{\rho}_{m,2s;2\sigma} = \frac{\gamma_{m,2\sigma}}{\gamma_{m,2s}} \frac{2-\delta_{s,0}}{2-\delta_{\sigma,0}} |\overleftarrow{r}_{m,2s;2\sigma}|^2$$

$$\overleftarrow{\tau}_{m,2s;2\sigma} = \frac{\gamma_{m,2\sigma}}{\gamma_{m,2s}} \frac{2-\delta_{s,0}}{2-\delta_{\sigma,0}} |\overleftarrow{t}_{m,2s;2\sigma}|^2$$

The total reflection and transmission coefficients $\rho_{m,2s}$, $\tau_{m,2s}$, $s = 0,1,\ldots,N^{(s)}$ are obtained simply by summing over all cut-on modes, i.e.,

$$\vec{\rho}_{m,2s} = \sum_{\sigma=0}^{N^{(s)}} \vec{\rho}_{m,2s;2\sigma}, \quad \vec{\tau}_{m,2s} = \sum_{\sigma=0}^{N^{(s)}} \vec{\tau}_{m,2s;2\sigma}, \text{ etc.}$$

The *power attenuation* or *insertion loss* in decibels for downstream and upstream sound transmission is then

$$\Delta\vec{P} = -10 \log_{10}(\vec{\tau}_{m,2s}) \text{ and } \Delta\overleftarrow{P} = -10 \log_{10}(\overleftarrow{\tau}_{m,2s})$$

Contrary to the no-flow situation (cf. Ref. 23) the absorption coefficient $\alpha_{m,2s}$ generally is not $1-\rho_{m,2s}-\tau_{m,2s}$. Only part of the acoustic power is absorbed by the liner while the remainder is used up for sustaining the formation of the vortex sheet similar to the analogous situation of a subsonic jet issuing from a pipe[18,29] or the sound transmission through blade rows[30] and past semi-infinite plates.[8,13]

The reciprocity theorem is not valid any longer in its original form. However, for the case of vanishing displacement jumps at $x = 0,l$ Howe's reverse flow reciprocity theorem[31] applies in the form (see Ref. 32 for the equivalent no-flow formulation)

$$(2-\delta_{m,2s})\gamma_{m,2\sigma} \frac{\hat{\vec{R}}_{m,2\sigma}(+U_\infty)}{\hat{\vec{E}}_{m,2s}(+U_\infty)} = (2-\delta_{m,2\sigma})\gamma_{m,2s} \frac{\hat{\overleftarrow{R}}_{m,2s}(-U_\infty)}{\hat{\overleftarrow{E}}_{m,2\sigma}(-U_\infty)}$$

$$(2-\delta_{m,2s})\gamma_{m,2\sigma} \frac{\hat{\vec{T}}^{*}_{m,2\sigma}(+U_\infty)}{\hat{\vec{E}}_{m,2s}(+U_\infty)} = (2-\delta_{m,2\sigma})\gamma_{m,2s} \frac{\hat{\overleftarrow{R}}_{m,2s}(-U_\infty)}{\hat{\overleftarrow{E}}^{*}_{m,2\sigma}(-U_\infty)}$$

Because of symmetry the additional relations

$$\frac{\hat{\vec{R}}_{m,2s}(-U_\infty)}{\hat{\vec{E}}_{m,2\sigma}(-U_\infty)} = \frac{\hat{\vec{T}}^{*}_{m,2s}(+U_\infty)}{\hat{\vec{E}}^{*}_{m,2\sigma}(+U_\infty)}$$

$$\frac{\hat{\vec{R}}_{m,2s}(-U_\infty)}{\hat{\vec{E}}^{*}_{m,2\sigma}(-U_\infty)} = \frac{\hat{\vec{T}}^{*}_{m,2s}(+U_\infty)}{\hat{\vec{E}}_{m,2\sigma}(+U_\infty)}$$

are valid and all together provide a valuable check of the numerical calculations. The important restriction of Howe's reverse flow theorem to situations with vanishing particle displacement at $x = 0$ and $x = l$ was first noticed by Möhring and Eversman.[26]

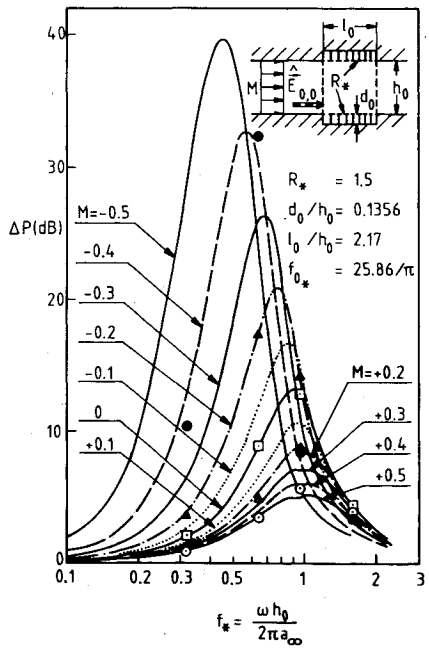

Fig. 3 Single-element liner: comparison with theory of Ref. 25.

Numerical Results

The purpose of this section is twofold. First, we want to compare the present solution with previous theoretical and experimental results, and second we try to determine which feature of the solution shows large enough differences for different choices of edge conditions such that it could be used to determine experimentally the physically correct edge conditions.

Power Attenuation Results

The quantity which, in general, gives the best picture of the quality of a liner is the power attenuation. Since several parameter studies already exist (e.g., Refs. 22 and 23), only one numerical example is shown here. Figure 3 extends the trend study of Ref. 23 to mean flows and, at the same time, provides a comparison with the recent singularity method results.[25] Depicted is the sound attenuation as a function of frequency number f_* with the mean flow Mach number varying between -0.5 and $+0.5$. For the impedance, the cross-over frequency model was used as in Refs. 23 and 25 with R_* being the dimensionless facing sheet resistance, $d = d_0/L_{\text{ref}}$ the dimensionless cavity depth, and f_{0*} the dimensionless cross-over frequency.

Figure 3 was evaluated by using the edge conditions A and keeping only two attenuated modes in the truncated infinite system of equations. The results of Ref. 25 are marked by symbols with fair agreement between the two solutions. For $M = \pm 0.4$ the solution was also evaluated for the edge conditions B and D with almost identical results. In the latter case D the exponentially increasing instability mode was neglected. A plausibility argument for this can be given by modifying some ideas of Möhring and Rahman[14] as mentioned in the Introduction. The nonlinear terms in the real problem, which we neglected in our model problem, would appear as source terms in the convected wave equation, Eq. (1). They alter the solution such that no unstable mode is excited a certain distance away from the upstream liner edge. As a first approximation we set the amplitude of the instability mode equal to zero in the whole field hoping that the overall error is not too large.

Once the reflection and transmission factors can be computed for a single finite length section, axially segmented multi-element liners can be evaluated by using the principle of modal superposition. Figure 4 shows a comparison with the

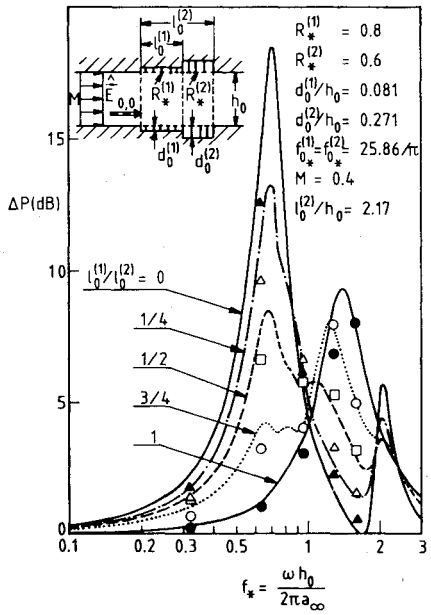

Fig. 4 Two-element liner: comparison with theory of Ref. 25.

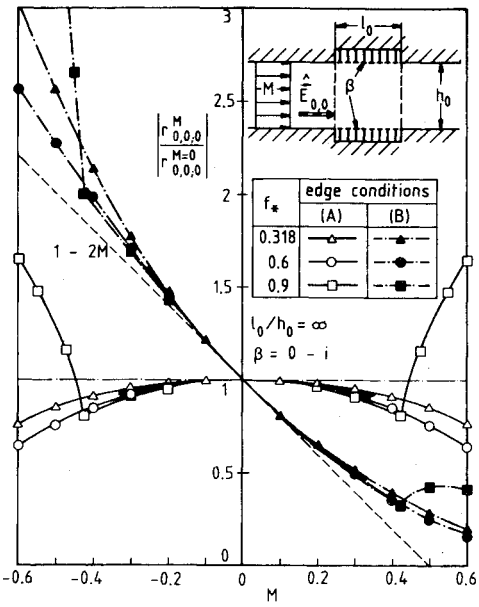

Fig. 6 Reflection factor for lossless liner: influence of frequency f_*.

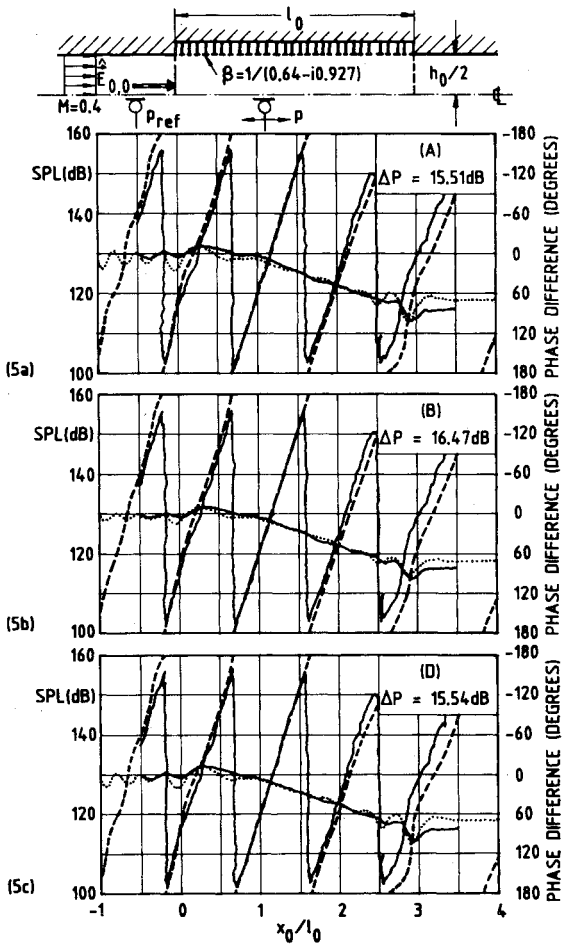

Fig. 5 Axial pressure traverse: comparison with experiment of Ref. 10 for edge conditions A, B, and D.

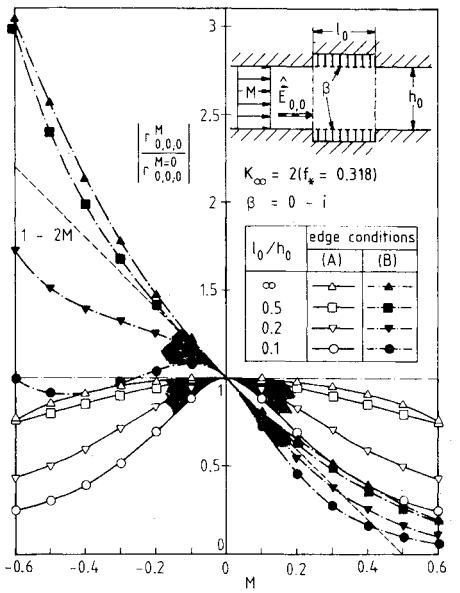

Fig. 7 Reflection factor for lossless liner: influence of liner length l_0.

two-element example of Ref. 25. Again, only two attenuated modes were kept in the truncated system as well as in the modal procedure.

Axial SPL-Traverse Results

In an experiment usually the local sound pressure is measured in the form of an axial SPL-traverse (cf. Ref. 10) and Fig. 5 shows a comparison of the present solution with such traverses (solid lines). For our chosen example the admittance is $1/(0.64 - i0.927)$, $K_\infty = 10.16$ ($f_* = 1.617$), and $M = 0.4$. The lined section extends from $x_0/h_0 = 0$ to 3 and, at the reference position $x_0/h_0 = -0.5$, the values of the SPL and the corresponding phase were taken to be 130 dB and -60 deg, respectively. According to the experimental measurements only the fundamental mode was excited and five attenuated modes were kept in our calculation. Figures 5a and 5b show the results for the edge conditions case A and case B, respectively. Even though in this noncausal formulation all modes were counted as decaying modes, the mode corresponding to the instability eigenvalue (i.e., $\lambda_{0,10} = 97.6474 + i36.7717$) had to be discarded. The reason is that the corresponding soft wall eigenfunction Eq. (40) not only varied quite rapidly over the duct cross section but also reached extraordinarily large values at the downstream liner end. In previous mode matching solutions (cf. Refs. 10 and 11) this mode was always omitted but, contrary to the causal solution, it is not clear why this should be done here. The causal solution corresponding to edge conditions D is shown

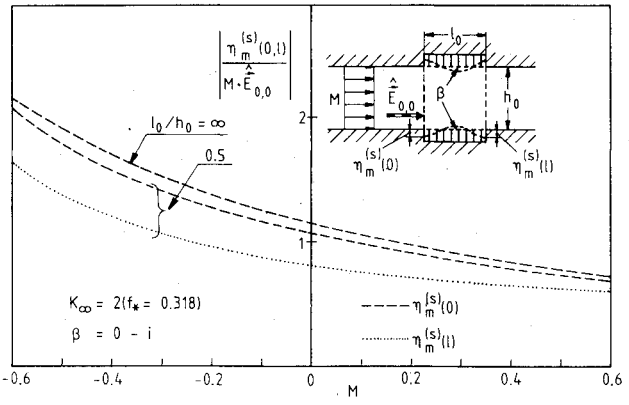

Fig. 8 Edge conditions B: liner displacement sheet jumps $\eta_m^{(s)}(0)$ and $\eta_m^{(s)}(l)$ for lossless liner.

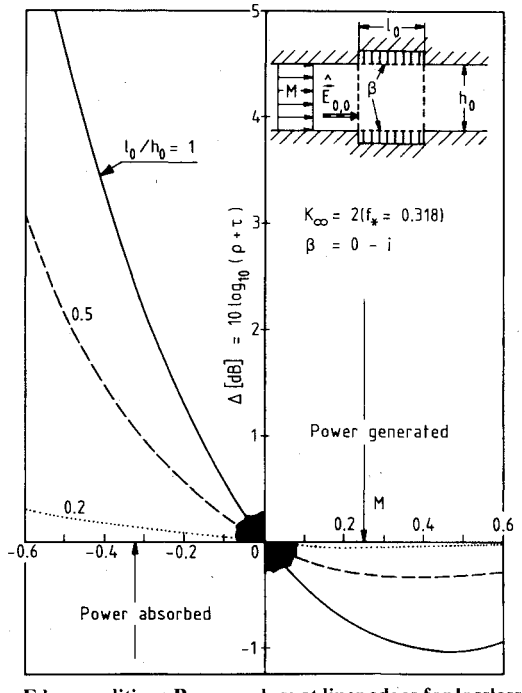

Fig. 9 Edge conditions B: power loss at liner edges for lossless liner.

in Fig. 5c with the amplitude of the increasing instability mode set equal to zero. All three solutions shown in Fig. 5 are fairly close to each other. The solution corresponding to C was way off and is not depicted.

Reflection Factor Results

Essentially, the power attenuation and pressure traverse results are of no help in deciding about the physically correct edge conditions. Contrary to this, the reflection factor $r_{m,2s;2n}$, usually of minor importance, shows strikingly differing results for different edge conditions. Figures 6 and 7 show the absolute values of the ratio $r^M_{0,0;0}/r^{M=0}_{0,0;0}$ for a "lossless" liner (i.e., with purely imaginary admittance) as investigated by Möhring and Eversman.[26] In Ref. 26 the mode matching method was applied (corresponding to our edge conditions B) and the result behaves like $1-2M$ for small M. Contrary to this we see that the singularity result (corresponding to our edge conditions A) is symmetric with respect to M.

Figure 8 indicates the continuous dependence of the displacement sheet jumps $\eta_m^{(s)}(0)$ and $\eta_m^{(s)}(l)$ on the Mach number starting with $M=0$ if conditions B are used. Lossless liners are of no practical importance but they are of theoretical interest because they show clearly that, depending

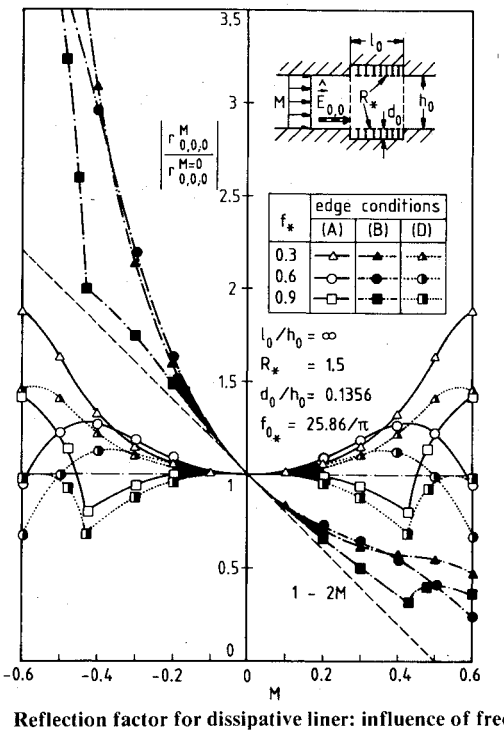

Fig. 10 Reflection factor for dissipative liner: influence of frequency f_*.

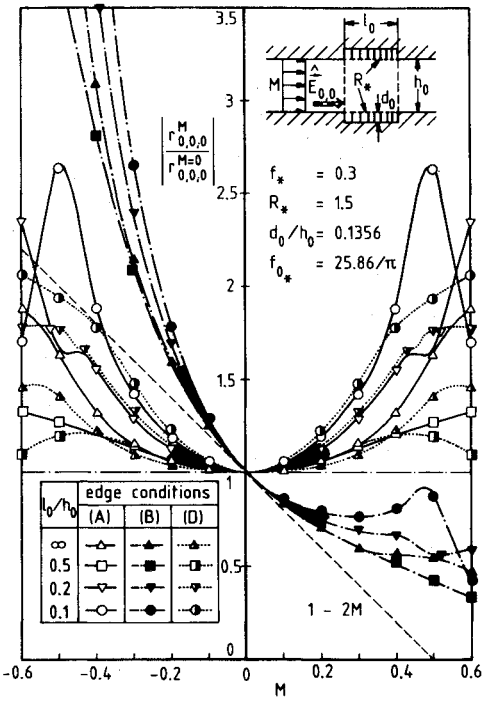

Fig. 11 Reflection factor for dissipative liner: influence of liner length l_0.

on the chosen edge conditions, additional power can be absorbed or generated at the edges. This is evident from Fig. 9 for the edge conditions B. For conditions A no power is generated or absorbed in the lossless case and to a certain extent this difference can be observed in Fig. 5 where the mode matching result (Fig. 5b) gives higher power attenuation.

Real liners are dissipative and corresponding examples for the reflection factor are shown in Figs. 10 and 11 with qualitatively similar results as for lossless liners. Also plotted is the solution for edge conditions D. The differing behavior

of the reflection factor for different edge conditions should allow for experimental decision about the physically appropriate edge conditions, at least whether B or A and D are more realistic.

Conclusion

The solution of the finite length liner problem is shown to be not unique and depends on the imposed edge conditions. The most rational choice appears to be the "causal" solution corresponding to edge conditions D. These require the application of the Kutta condition at the upstream edge and a square root singularity of the liner displacement sheet at the downstream edge. In addition, the amplitude of the exponentially increasing instability mode in the lined section has to be set to zero as a first approximation to the nonlinear situation. Also indicated is how measurements of the reflection factor can be used to make a more definite decision about the physically most appropriate edge conditions.

Acknowledgments

This research was initiated while the first author held an NRC Research Associateship at NASA Langley Research Center. This financial support, the kind hospitality at the Aeroacoustics Branch of NASA Langley under D. L. Lansing, as well as the stimulating and helpful discussions with J. C. Hardin, W. R. Watson, and T. L. Parrott of the Aeroacoustics Branch are gratefully acknowledged. We are also especially indebted to Prof. W. Eversman for supplying us with a copy of his eigenvalue routine in addition to his valuable advice.

References

[1] Baumeister, K. J., "Evaluation of Optimized Multisectioned Acoustic Liners," *AIAA Journal*, Vol. 17, Nov. 1979, pp. 1185-1192.

[2] Nayfeh, A. H., Kaiser, J. E., and Telionis, D. P., "Acoustics of Aircraft Engine-Duct Systems," *AIAA Journal*, Vol. 13, Feb. 1975, pp. 130-153.

[3] Vaidya, P. G. and Dean, P. D., "State of the Art of Duct Acoustics," AIAA Paper 77-1279, Oct. 1977.

[4] Ffowcs Williams, J. E., "Aeroacoustics," *Annual Review of Fluid Mechanics*, Vol. 9, Annual Reviews Inc., Palo Alto, 1977, pp. 447-468.

[5] Tester, B. J., "The Propagation and Attenuation of Sound in Lined Ducts Containing Uniform or 'Plug' Flow," *Journal of Sound and Vibration*, Vol. 28, May 1973, pp. 151-203.

[6] Orszag, S. A. and Crow, S. C., "Instability of a Vortex Sheet Leaving a Semi-Infinite Plate," *Studies in Applied Mathematics*, Vol. 49, June 1970, pp. 167-181.

[7] Munt, R. M., "The Interaction of Sound with a Subsonic Jet Issuing from a Semi-Infinite Cylindrical Pipe," *Journal of Fluid Mechanics*, Vol. 83, Dec. 1977, pp. 609-640.

[8] Rienstra, S. W., "Edge Influence on the Response of Shear Layers to Acoustic Forcing," Ph.D. Thesis, Technische Hogeschool Eindhoven, June 1979.

[9] Zorumski, W. E., "Acoustic Theory of Axisymmetric Multisectioned Ducts," NASA TR R-419, May 1974.

[10] Sawdy, D. T., Beckemeyer, R. J., and Patterson, J. D., "Analytical and Experimental Studies of an Optimum Multisegment Phased Liner Noise Suppression Concept," NASA CR-134960, May 1976.

[11] Kraft, R. E., "Theory and Measurement of Acoustic Wave Propagation in Multi-Segmented Rectangular Flow-Ducts," Ph.D. Thesis, University of Cincinnati, 1976.

[12] Jones, D. S. and Morgan, J. D., "The Instability of a Vortex Sheet on a Subsonic Stream under Acoustic Radiation," *Proceedings of the Cambridge Philosophical Society*, Vol. 72, 1972, pp. 465-488.

[13] Crighton, D. G. and Leppington, F. G., "Radiation Properties of the Semi-Infinite Vortex Sheet: The Initial-Value Problem," *Journal of Fluid Mechanics*, Vol. 64, June 1974, pp. 393-414.

[14] Möhring, W. and Rahman, S., "Sound Generation in a Flow Near a Compliant Wall," *Journal of Sound and Vibration*, Vol. 66, Oct. 1979, pp. 557-564.

[15] Swinbanks, M. A., "The Sound Field Generated by a Source Distribution in a Long Duct Carrying Sheared Flow," *Journal of Sound and Vibration*, Vol. 40, May 1975, pp. 51-76.

[16] Mani, R., "Sound Propagation in Parallel Sheared Flows in Ducts: The Mode Estimation Problem," *Proceedings of the Royal Society, London*, Series A, Vol. 371, June 1980, pp. 393-412.

[17] Munt, R. M., "Acoustic Transmission Properties of a Jet Pipe with Subsonic Jet Flow: (I) The Cold Jet Reflection Coefficient," Rept., Mathematics Department, The University, Dundee, March 1978.

[18] Munt, R. M., "Acoustic Transmission Properties of a Jet Pipe with Subsonic Jet Flow: (II) The Cold Jet Radiated Power," Rept., Mathematics Department, The University, Dundee, Sept. 1978.

[19] Nilsson, B. and Brander, O., "The Propagation of Sound in Cylindrical Ducts with Mean Flow and Bulk-Reacting Lining—I. Modes in an Infinite Duct," *Journal of the Institute of Mathematics and its Application*, Vol. 26, Nov. 1980, pp. 269-298.

[20] Nilsson, B. and Brander, O., "The Propagation of Sound in Cylindrical Ducts with Mean Flow and Bulk-Reacting Lining—II. Bifurcated Ducts," *Journal of the Institute of Mathematics and its Applications*, Vol. 26, Dec. 1980, pp. 381-410.

[21] Noble, B., *Methods Based on the Wiener-Hopf Technique for the Solution of Partial Differential Equations*, Pergamon Press, London, 1958.

[22] Ko, S.-H., "Sound Attenuation in Lined Rectangular Ducts with Flow and its Application to the Reduction of Aircraft Engine Noise," *Journal of the Acoustical Society of America*, Vol. 50, Dec. 1971, pp. 1418-1432.

[23] Koch, W., "Attenuation of Sound in Multi-Element Acoustically Lined Rectangular Ducts in the Absence of Mean-Flow," *Journal of Sound and Vibration*, Vol. 52, June 1977, pp. 459-496.

[24] Eversman, W., "Initial Values for the Integration Scheme to Compute the Eigenvalues for Propagation in Ducts," *Journal of Sound and Vibration*, Vol. 50, Jan. 1977, pp. 159-162 (Errata: *Journal of Sound and Vibration*, Vol. 53, Aug. 1977, p. 595).

[25] Namba, N. and Fukushige, K., "Application of the Equivalent Surface Source Method to the Acoustics of Duct Systems with Non-Uniform Wall Impedance," *Journal of Sound and Vibration*, Vol. 73, Nov. 1980, pp. 125-146.

[26] Möhring, W. and Eversman, W., "Conversion of Acoustic Energy by Lossless Liners," *Journal of Sound and Vibration*, Vol. 82, June 1982, pp. 371-381.

[27] Crighton, D. and Innes, D., "Analytical Models for Shear-Layer Feed-Back Cycles," AIAA Paper 81-0061, Jan. 1981.

[28] Howe, M. S., "The Influence of Mean Shear on Unsteady Aperture Flow, with Application to Acoustical Diffraction and Selfsustained Cavity Oscillations," *Journal of Fluid Mechanics*, Vol. 109, Aug. 1981, pp. 125-146.

[29] Bechert, D. W., "Sound Absorption Caused by Vorticity Shedding, Demonstrated with a Jet Flow," *Journal of Sound and Vibration*, Vol. 70, June 1980, pp. 389-405.

[30] Koch, W., "Ergänzende Untersuchungen zum Schalldurchgang durch ein zweidimensionales Plattengitter," DFVLR-AVA Internal Rept. IB 251-78 A01, Jan. 1978.

[31] Howe, M. S., "The Generation of Sound by Aerodynamic Sources in an Inhomogeneous Steady Flow," *Journal of Fluid Mechanics*, Vol. 67, Feb. 1975, pp. 597-610.

[32] Cho, Y.-C., "Reciprocity Principle in Duct Acoustics," *Journal of the Acoustical Society of America*, Vol. 67, May 1980, pp. 1421-1426.

[33] Streater, R. F. and Wightman, A. S., "Die Prinzipien der Quantenfeldtheorie," Bibliographisches Institut AG, Mannheim, 1969, pp. 100-103.